Elevated fire danger conditions associated with foehn-like winds in southeastern Australia

J. J. Sharples [1,4], G.A. Mills [2,4], R.H.D. McRae [3,4], R.O. Weber [1,4]

1. School of Physical, Environmental and Mathematical Sciences, University of New South Wales at the Australian Defence Force Academy. Canberra, Australia.
2. Centre for Australian Weather and Climate Research. Melbourne, Australia
3. Australian Capital Territory Emergency Services Agency. Canberra, Australia.
4. Bushfire Cooperative Research Centre. Melbourne, Australia.

Draft: 22nd January 2009

Abstract

Bushfires in southeastern Australia are a serious environmental problem, which consistently cause loss of life and damage to property and other assets. Understanding synoptic processes that can lead to dangerous fire weather conditions throughout the region is therefore an important undertaking aimed at improving community safety, protection of assets and fire suppression tactics and strategies. In southeastern Australia severe fire weather is often associated with dry cool changes or coastally modified cold fronts. Less well known, however, are synoptic cases that can occur in connection with the topography of the region, such as cross-mountain flows and foehn-like winds, which can also lead to abrupt changes in fire weather variables that ultimately result in locally elevated fire danger. This paper focuses on foehn-like occurrences over the southeastern mainland, which are characterised by warm, dry winds on the lee side of the Australian Alps. The characteristics of a number of foehn-like occurrences are analysed based on observational data and the predictions of a numerical weather model. The analyses confirm the existence of a foehn effect over parts of southeastern Australia and suggest that its occurrence is primarily due to the partial orographic blocking of relatively moist low-level air and the subsidence of drier upper-level air in the lee of the mountains. The regions prone to foehn occurrence, the influence of the foehn on fire weather variables and the connection between the foehn and mountain waves are also discussed.

Keywords: foehn, southeastern Australia, fire weather, fire danger, mountain wave

1. Introduction

The potential for the occurrence and development of bushfires is dependent upon the interaction of fuels with variables such as air temperature, atmospheric dryness and wind speed. Typically, these variables are combined with information on drought effects to produce a fire danger rating or fire danger index, which provides a measure of the chance of a fire starting in a particular fuel, its spread and difficulty to control and the damage it is likely to cause (Chandler et al., 1983). A number of different fire danger indices have been devised around the world, each reflecting the different climates and fuel types in which they are employed (McArthur, 1966; 1967; Rothermel, 1972; Noble et al., 1980; Sneeuwjagt and Peet, 1985; Van Wagner and Pickett, 1985; Gill et al., 1987; Beck, 1995; Forestry Canada Fire Danger Group, 1992). Despite the inherent differences in their design and implementation, all fire danger rating schemes generally agree that hotter, drier and windier conditions will result in higher levels of fire danger, all other factors being equal.

Consequently, fire weather forecasts should aim to accurately predict changes in near-surface air temperature, relative humidity and wind speed, both in space and in time. Understanding the synoptic processes through which such changes can occur is therefore an important problem for meteorologists, particularly those tasked with providing fire weather information to land and emergency managers. The development of synoptic models to assist in forecasting these changes is thus a key requirement in improving bushfire control and risk management practices.

In southeastern Australia the synoptic archetypical severe fire weather day is that of the dry "cool change", or coastally modified cold front (see for example Bond et al., 1968; Mills, 2002; Mills, 2005). In such events the hot, dry, gusty northwesterly winds in the pre-frontal air mass cause extreme fire danger. The abrupt wind change associated with the passage of these fronts also leads to major spread of the fire after the wind change (Cheney et al., 2001) and this effect is particularly exacerbated if the front extends for some depth in the troposphere (Mills, 2005) as this can lead to sustained wind speeds after the frontal passage. Similar ingredients are found in the southwest of Western Australia with the passage of the eastward-propagating west-coast troughs, while along the east coasts of Tasmania and New South Wales frontal passages are also a typical factor in generating extreme fire weather, albeit with substantial modification due to topography and land-sea heating contrasts (e.g. Mills and Pendlebury, 2003; Mills, 2007).

Less well known, however, are synoptic cases that occur in connection with the topography of the eastern Australian mainland and Tasmania, which can also lead to abrupt spatiotemporal changes in fire weather variables that ultimately result in locally elevated fire danger. Some of these cases are associated with cross-mountain flows and foehn-like occurrences, the latter of which are characterised by warm, dry winds on the lee side of mountain ranges; the warmth and dryness of the air being due to adiabatic compression of the air descending the mountain slopes (Huschke, 1959; WMO, 1992). While some knowledge about Australian foehn winds does exist, it has not been widely disseminated and generally stems from brief accounts that are based on experience rather than detailed scientific studies. For example, some of these simply note the possibility of higher temperatures, or reduced fog occurrence in the lee of the ranges in some instances (P. Riley, personal communication). An exception is the study by Marsh (1987) on the extreme fire weather of the 6^{th} of November 1982 in southeast Tasmania. Marsh (1987) notes the possibility of a large-scale 'foehn-type' downslope flow contributing to the extreme fire weather of the day. However, on the whole, the extent to which the foehn effect applies over Australia's mountainous regions, the mechanisms behind it and how it might affect local fire danger levels appear to be largely open problems.

Internationally, the foehn effect occurs in the vicinity of many mountainous regions and produces characteristically warm, dry down-slope winds called foehn winds. Of particular note, in the context of fire weather, are the Santa Ana winds of southern California. Keeley (2004) found that the autumn foehn (Santa Ana) in southern California was a key driver in determining area burned, over-riding most other climate signals. Foehn winds also feature significantly as drivers of severe fire weather in Europe. Carrega (1991) discusses occurrences of catastrophic fires near the French-Italian border driven by westerly foehn winds, while Conedera et al. (1996) report that in southern Switzerland the main time for forest fires is during north foehn occurrences. The 1997 fire season in particular, serves as an example (Conedera et al., 1998). Foehn winds are also routinely mentioned in New Zealand fire weather assessments due to the effect that they have on humidity levels in the lee of the main mountain ranges (Salinger, et al., 2000; Salinger and Porteous, 2002; Gosai and Salinger, 2003; 2004; 2005), and have been connected with elevated forest fire risk in Japan (Kondo and Kuwagata, 1992;

Ninomiya et al., 1985) and certain parts of Korea (Lim, 2002), despite the milder topography encountered there.

Generally speaking, foehn winds are caused by the adiabatic compression of air flowing down the lee slopes of mountain barriers (Huschke, 1959; Barry, 1992; WMO, 1992; Whiteman, 2000). Their occurrence has been attributed to two main mechanisms. The first involves the forced ascent of moist air over a mountain barrier. The moist air cools as it rises, ultimately resulting in condensation and precipitation. The precipitation removes much of the moisture from the air mass and the latent heat of condensation raises the temperature of the air. The drier air is then warmed further due to adiabatic compression as it descends the lee slopes (Hann, 1866; Hann 1867; Barry, 1992, Whiteman, 2000). This type of foehn can be referred to as thermodynamically-driven. The second foehn mechanism involves the blocking of lower-level air by a mountain barrier, with drier upper air flowing down to replace it in the lee of the mountains. As the drier air from above descends the lee slopes it is warmed by adiabatic compression. This type of foehn is a consequence of blocking of air flows by the mountains, which is essentially a mechanical effect, and so will be referred to as mechanically-driven. Instances of mechanically-driven foehn winds have been studied by Cook and Topil (1952), Brinkmann (1973; 1974), Lockwood (1962), Seibert, (1990) and Ustrnul (1992). It is typical for the mechanically-driven foehn to occur in association with a vertically propagating lee mountain wave (Lockwood, 1962; Drobinski et al., 2007; Drechsel and Mayr, 2008).

Throughout the literature a number of criteria have been used to distinguish 'foehn conditions' (Drobinski et al., 2007; Sharples, 2009). Commonly though, three criteria are used to distinguish foehn conditions at stations in the lee of mountains (Osmond, 1941; Frey, 1957). They are: surface winds blowing from the direction of the mountains, an abrupt rise in air temperature in the lee of the mountains and an accompanying reduction in atmospheric moisture. Synoptic criteria can also be used to distinguish foehn conditions (Brinkmann, 1970; 1971; Vergeiner, 1971; Beer, 1974; Hoinka 1985; Barry 1992; McGowan and Sturman 1996; Gohm et al., 2004). Furthermore, foehn conditions are often accompanied by distinctive cloud formations. While these cloud formations often bear their own local names (e.g. the 'chinook arch'), we may refer to them in generic terms as the foehn wall and foehn arch. The foehn wall is an orographic cloud band that forms along the ridge tops of mountain ranges due to condensation of moisture as the air is lifted up the windward slopes, while the foehn arch is an extensive layer of altostratus cloud that forms downwind of the mountains in the rising portion of a standing lee mountain wave. Typically, a band of clear air called the foehn gap can be observed between the wall and arch clouds. Examples of a foehn arch and foehn gap over southeastern Australia can be seen in figure 1.

In this paper we focus on the mountainous region of southeastern Australia, known as the Australian Alps, and present a study of foehn-like conditions that occur to their east and southeast. The study uses data from automatic weather stations combined with numerical modelling, using the Bureau of Meteorology's meso-LAPS 0.05^{o} (approx. 5km) resolution numerical weather model, to select and investigate a number of candidate events. In addition to addressing the question of the existence of foehn winds in southeastern Australia, the atmospheric mechanisms for foehn-like winds are also investigated. Based on the analyses we discuss precursor conditions for foehn-like occurrences and their seasonality, which taken together provide a basis for developing better forecast techniques and a southeast Australian foehn climatology.

We note that although the motivation for this work derives from the need for a more formal understanding of synoptic processes that can result in elevated fire danger in southeastern Australia, the study also provides information of general meteorological interest. This is particularly the case in relation to downslope wind storms and strong winds and turbulence associated with mountain wave troughs impacting the ground in the lee of the Australian Alps. In this regard the study provides information that is useful in non-fire weather applications such as the dispersion of pollution, light and recreational aviation and scheduling snow making at ski resorts (Drechsel and Mayr, 2008).

We begin in section 2 by identifying a number of candidate foehn-like events observed over southeastern Australia in 2000, 2007 and 2008 and discussing the data and methods used in the study. Section 3 presents an analysis of the characteristics of the candidate events based on weather observations recorded at a number of automatic weather stations, as well as analyses of the atmospheric structure using the meso-LAPS numerical weather model. We then close the paper with a discussion of the results and their implications for bushfire risk management in southeastern Australia.

2. Candidate events, data and methods

Foehn winds are principally characterised by warming and drying in regions to the lee of the main mountain ranges, in this case the Australian Alps. Their occurrence can also be indicated by the presence of distinct cloud formations, as mentioned above. Based on these premises, a cursory examination of satellite imagery and observations of temperature, relative humidity and dew point temperature, over the period from May 2007 to November 2008, identified a number of candidate foehn-like events. Six of these events were selected for more detailed analysis: the 29th of May 2007, the 2nd of April 2008, the 28th of April 2008, the 19th and 20th of September 2008, and the 27th of October 2008. These six events were chosen because of their proximity to the official fire season in southeastern Australia (typically October–April); because they displayed pronounced, spatially coherent differences in temperature and humidity between regions to the lee and windward sides of the mountains; and/or because associated satellite imagery (visual and water vapour) displayed features that were consistent with foehn occurrence.

In addition, we also analysed two events that took place on the 29th of September 2000 and the 1st of October 2000. These two events were brought to the attention of the authors by colleagues in the Bureau of Meteorology who had noted their effects on the Olympic rowing/canoeing events during the 2000 games (T. Bannister, personal communication).

To facilitate a more in-depth analysis of the events described above, observational data from a number of automatic weather stations were obtained from the Bureau of Meteorology. The data included measurements of dry-bulb temperature, relative humidity, dew point temperature and wind speed, direction and gust. The stations utilised in the study are listed in table 1, along with their locations, elevations and monthly mean maximum temperatures. The position of these stations in relation to the major topographic features of the southeast Australian mainland can also be seen in figure 2. To supplement the observational analyses of the candidate events, analyses using the 0.05^{o} resolution numerical weather prediction model meso-LAPS (Puri et al., 1998) were also undertaken to demonstrate the evolving 3-dimensional atmospheric structures associated with the occurrence of these foehn-like events at the surface.

3. Case studies

In this section we provide a detailed account of the meteorological observations surrounding two of the candidate events (29th May 2007 and 27th October 2008). In particular we focus on the evolution of the events through analysis of temperature, relative humidity, dew point and wind observations recorded at lee stations, located in the relevant areas, compared with those recorded at windward and other non-lee stations. In addition we discuss the atmospheric dynamics associated with these two events, as given by the meso-LAPS model. The observations and model predictions for the other six events will only be discussed briefly in sections 3.3 – 3.8.

3.1 29th May 2007

Interpolated surfaces of temperature, relative humidity and dew point temperature at 15:00 AEST can be seen in figures 3a, 3b and 3c, respectively. Figure 3d shows the corresponding map of McArthur Mark 5 Forest Fire Danger Rating (McArthur, 1966;

Noble et al., 1980). Figure 3a indicates a region of warmer temperatures (~ 26 ^{o}C) along the Victorian coast to the south of the mountains (the Gippsland region). This region intersects with a broader region of depressed dew point (figure 3c) and coincides with a region of anomalous relative humidity (figure 3b). Figure 3d indicates that the region has significantly elevated forest fire danger rating (reaching levels classified as 'high', i.e. 12 $\leq$ FFDR $\leq$ 24), when compared to other parts of the coast.

The evolution of the event at East Sale Airport, Melbourne Airport and Wangaratta can be seen in figures 4a, 4b and 4c, which show time series of temperature, relative humidity and dew point. Figure 4a shows that for the period of 11:30 to 18:00 AEST, the temperature at East Sale Airport was between 4^{o}C and 9^{o}C higher than the corresponding temperatures at Melbourne and Wangaratta, while figure 4b indicates that for the same period, the relative humidity at East Sale was between 20% and 65% lower than that at Melbourne and Wangaratta.

Temperature at East Sale started to rise after midnight and the higher temperatures (peaking at 24.5 ^{o}C) were seen to persist for several hours after noon, when the temperatures at the other two stations began to fall. In fact the temperature at East Sale stayed above 20 ^{o}C until after 17:00, when the temperatures at Melbourne and Wangaratta were just above 12 ^{o}C. The maximum temperatures recorded at Melbourne and Wangaratta were only about 1-2 ^{o}C higher than their respective average temperatures, whereas the maximum temperature of 24.5 ^{o}C, recorded at East Sale was approximately 8-9 ^{o}C higher than the average for May-June (see table 1). The winds at East Sale, at the times when the elevated temperatures were recorded, were from the north to northeast with speeds of 20-30 km h^{-1}, gusting to over 50 km h^{-1} in the middle of the day. In northwesterly synoptic-scale wind flows the combination of the lee-trough effect and the land-sea temperature contrast acts to produce a marked northeasterly flow along the Gippsland coast. Examples of this effect are given in Huang and Mills (2006), pp47-51.

The differences in relative humidity were most extreme at approximately 15:00 when the relative humidity was 31% at East Sale and around 80-90% at Melbourne and Wangaratta. These differences in relative humidity are of course driven in part by the corresponding differences in temperature, but the dew point time series in figure 4c also indicate that the air at East Sale was drier, in absolute terms, than that at Melbourne and Wangaratta, with a dew point 2-8^{o}C lower than what was recorded at those two stations. Moreover, the dew point time series for East Sale shows the opposite trend to the time series for the other two stations.

Anomalously warm and dry conditions were also observed at other stations in the lee of the main range. For example, Bairnsdale, Orbost, Latrobe Valley and Mt Nowa Nowa recorded maximum temperatures of 24 ^{o}C, 24.2 ^{o}C, 22.9 ^{o}C and 22.6 ^{o}C, respectively, all of which are approximately 7-8^{o}C above the average maximum temperatures for that time of year (table 1). Relative humidity minima, recorded between 15:00 and 16:30 at these stations, were around 34-37%, similar to the East Sale observations. The location of this warm and dry region in the lee of the ranges is consistent with the position of the foehn gap and foehn arch seen in figure 1, which shows the situation at around 12:30 AEST.

Figure 5 shows meso-LAPS model output of the ω-field at the 500hPa level. The variable ω is defined by $dp = \omega\ dt$, where p denotes air pressure and t denotes time, so that positive and negative values of ω indicate descending and ascending air, respectively. A large region of descending air can be seen over the main ranges with a corresponding region of ascending air in the lee. This pattern is consistent with a large-scale topographically induced gravity wave, which forms as upper air descends in the lee of the main range, replacing lower level windward air that has been blocked by the mountains. The existence of a vertically propagating gravity wave is confirmed by the vertical cross sections shown in figure 6. The horizontal extent of the cross sections is shown in plan view in the top left panel of figure 5. Note that the cross section extends beyond the bounds of the figure.

Figure 6a shows air descending above and in the lee of the mountains. The mixing ratio isopleths evident in figure 6b indicate that relatively moist lower-level air is being partially blocked by the mountain barrier and is being replaced in the lee by drier upper level air, mostly from the around the 800-900hPa layer. The isentropes in figure 6c portray the typical pattern expected for a vertically propagating gravity wave, while the projected wind vectors indicate strong downslope winds associated with the wave motion in the immediate lee of the mountains. This is consistent with observations at East Sale, Bairnsdale and Orbost, which recorded wind gusts of 50-60 km h^{-1}. However, winds were strong over all of Victoria on the 29th of May, with winds at Shepparton gusting to 60 km h^{-1} and Melbourne Airport recording gusts of over 90 km h^{-1}, for example. The modelled atmospheric behaviour evident in figures 5 and 6 was seen to persist for several hours until about 18:00 AEST.

3.2 27th October 2008

The foehn-like dynamics observed on the 27th of October 2008 occurred in two stages; the first in the morning, associated with northerly winds and the second in the afternoon, associated with northwesterly winds. Interpolated surfaces of temperature, relative humidity and dew point temperature for 11:00 AEST can be seen in figures 7a, 7b and 7c, respectively. Figure 7a shows two localised regions of elevated temperature (≥ 30 ^oC) along the Gippsland coast of Victoria and to the southeast of the Australian Capital Territory. Figures 7b and 7c indicate that these two regions were also experiencing lower humidity levels, with relative humidity along the Gippsland coast less than 10%. Interpolated forest fire danger rating for 11:00 AEST can be seen in figure 7d, which indicates that fire danger rating on the Gippsland coast of Victoria was significantly elevated (FFDR $\approx$ 30) , particularly for the morning. Fire danger rating for this region falls into the 'very high' class ($24 \leq$ FFDR ≤ 50).

The second stage is typified by the interpolated surfaces of temperature, relative humidity, dew point temperature and fire danger rating for 15:00 AEST seen in figures 8a, 8b, 8c and 8d. Figures 8a and 8b show a region of elevated temperature (≥ 35 ^oC) and depressed relative humidity ($\leq$ 10%) in the lee of the ranges along the southern New South Wales coast. The fire danger rating surface in figure 8d again shows a corresponding region of elevated fire danger rating (FFDR $\approx$ 35).

The evolution of the event can be seen in the temperature, relative humidity and dew point time series for Bega, Orbost and Albury in figure 9. In figure 9a, the temperature trace at Orbost is seen to increase rapidly from 17.4 ^{o}C at 03:30 to 25.6 ^{o}C at 06:00 (around the time of sunrise). The temperature then continues to rise to 32 ^{o}C at 10:56 after which it quickly decreases with the passage of a cold front over the region. The maximum temperature of 32 ^{o}C is approximately 12 ^{o}C warmer than the average for Orbost for October-November. Just to the west, the temperature at Mt Nowa Nowa displayed a similar but less pronounced effect; temperature rose to 26 ^{o}C at 09:00, and the daily maximum of 26.6 ^{o}C was attained before noon. About three hours after the sharp temperature increase at Orbost, the temperature trace for Bega exhibits a significant increase from 13.1 ^{o}C at 05:30 to 32 ^{o}C at 10:06. The temperature at Bega then continues to increase to a maximum of 36 ^{o}C at 13:30, which is approximately 14 ^{o}C above the average maximum temperature for October-November. By contrast, on the upwind side of the mountains, Albury only experienced an increase in temperature of about 7 ^{o}C, reaching a maximum of 27.7 ^{o}C, which is only 3-4 ^{o}C above average. Merimbula and Moruya also exhibited patterns in their temperature traces similar to Bega. Merimbula increased from 12 ^{o}C at 06:30 to 26.1 ^{o}C at 10:30 and reached a maximum of 32.8 ^{o}C, about 11 ^{o}C above average. Moruya also increased rapidly from 13.3 ^{o}C at 07:00 to 30.5 ^{o}C at 10:00 and then to a maximum of 35.4 ^{o}C at 15:00, about 14 ^{o}C above average. In fact the temperature at Moruya stayed above 32 ^{o}C from 11:00 to 19:00. Similar but less pronounced effects were also observed at Green Cape, Bombala and Cooma. The warm events at both Bega and Orbost are ended by the passage of a cold front, the evolution of which can be seen in figure 10.

The relative humidity time series for Orbost and Bega in figure 9b exhibit changes that complement the changes in temperature just discussed. Orbost is seen to drop from 48% at 03:30 to 23% at 06:00, and then to 16% at 10:56 after which the relative humidity is observed to rapidly increase with the arrival of the cold front (figure 10). Mt Nowa Nowa also recorded a relative humidity of 14%, which persisted from 08:30 to 11:00. Similarly, Bega experienced a dramatic decrease in relative humidity from 99% at 07:00 to 15% at 10:30, and then to a minimum of 11% at 12:38. Relative humidity at Bega then remained between 11% and 15% until 17:30, after which the arrival of the cold front caused it to increase sharply. Moruya and Merimbula also experienced very low relative humidity. Relative humidity at Moruya dropped from 79% at 07:00 to 20% at 10:00 and then to a minimum of 13% at 15:00. During the period of 11:00 to 19:00 relative humidity at Moruya was between 13% and 16%. At Merimbula a similar effect was observed with relative humidity dropping from 91% at 07:00 to 36% at 10:30, and then to 15% and 16:30. In contrast the upwind relative humidity at Albury over a similar period only decreased from 39% to 18%, and did so much more slowly than at the other stations just discussed.

Figure 9c indicates that reduction in atmospheric moisture played a significant part in the lowered relative humidity discussed in the previous paragraph. At Orbost the dew point drops from 6.8 ^{o}C at 03:00 to 2.5 ^{o}C at 06:30, while nearby Mt Nowa Nowa recorded a minimum dew point temperature of -4 ^{o}C at 08:30. Figure 9c shows that Bega recorded a fall in dew point temperature from 14.6 ^{o}C at 09:00 to 1.6 ^{o}C at 11:00; the dew point then continued to fall to a minimum of 0.2 ^{o}C at 12:38. Similarly, Merimbula recorded a drop in the dew point from 13.6 ^{o}C at 09:00 to a minimum of 2.3 ^{o}C at 16:30, while Moruya recorded a fall from13 ^{o}C at 09:00 to a minimum of 2 ^{o}C at 12:49.

Wind data recorded at Orbost indicated that between 06:00 and 11:00 winds were relatively strong, north to north-northwesterly, with speeds between 24 and 37 km h^{-1}, gusting to 60 km h^{-1} (figures 10 and 11a). The period of increased temperature and decreased humidity therefore coincides with times when Orbost was in the immediate lee of the dominant topography. Similarly, the rapid increase in temperature and drop in humidity observed at Bega coincided with the onset of strong winds from between west-northwest and north-northwest (figures 10 and 11b), placing Bega in the lee of the mountains. Wind speeds at Bega increased from 7 km h^{-1} at 09:30 to 39 km h^{-1} at 13:30, with gusts recorded as high as 59 km h^{-1}. Winds at Bega began to abate after 17:30 with the onset of an easterly flow (figure 10).

Figure 12 shows output from meso-LAPS for 09:00 AEST on the 27th of October 2008; the 500 hPa level ω-field can be seen in figure 12a while vertical cross-sections of mixing ratio, potential temperature and projected wind vector can be seen in figures 12b and 12c. The horizontal extent of the cross-section is shown in plan view in figure 12a. Note that the cross-section extends beyond the bounds of the figure. Also note that the topographic shading in figure 12a is the same as in figure 5. In figure12a a region of descending air is evident over the Australian Alps to the north and northwest of Orbost at a time when Orbost was experiencing relatively warm and dry conditions. A region of upper-level ascending air can be seen in the immediate lee of the mountains, over Orbost. This again suggests the existence of a vertically propagating gravity wave over the affected region. Topographically induced wave structure is also evident in the cross-sections in figures 12b and 12c. Figure 12b indicates that moist windward air is being partially blocked by the topography and is being replaced by drier upper level air in the lee. The isentropes in figure 12c are consistent with the presence of a vertically propagating gravity wave causing strong downslope winds over the south coast of New South Wales. The projected wind vectors in figure 12c suggest that the downslope winds were quite strong, especially near the surface in the lee of the coastal escarpment. This is consistent with the strong winds recorded at Bega just before 11:00 AEST on the 27th of October 2008, evident in figure 11b.

3.3 29th September 2000

The contrast between conditions downwind on the southern New South Wales coast and the upwind region can be seen in table 2. The downwind stations exhibited an abrupt increase in temperature (~ 9^{o}C in two hours) and an associated decrease in relative humidity. Similar warming and drying were also observed further inland at Cooma, Braidwood, Canberra and Bombala. The increases in temperature and the associated decreases in relative humidity occurred in connection with a period of strong westerly to north-northwesterly winds with speeds of up to 50 km h^{-1}, gusting to 80 km h^{-1}.

A similar effect was also observed in the lee of the Blue Mountains region where temperature maxima at Penrith Lakes, Badgerys Creek, Bankstown Airport and Sydney Airport were approximately 10 ^{o}C above average. The elevated temperatures again coincided with the influx of significantly drier air. The winds were from the west to northwest, with speeds of 30-40 km h^{-1}, gusting to 60 km h^{-1}.

Numerical modelling using meso-LAPS indicated that the foehn-like conditions were again associated with blocking of moister low-level upwind air with relatively dry upper air descending the lee slopes of the ranges in connection with a topographically induced gravity wave.

3.4 1st October 2000

Elevated temperatures and depressed relative humidity were again recorded during the 1st of October 2000 on the southern New South Wales coast (table 2) and in the lee of the Blue Mountains. The events were characterised by strong westerly winds across both regions. Wind speeds in the lee of the Blue Mountains reached 55 km h^{-1} with gusts of 75 km h^{-1}, while on the south coast of New South Wales the wind speeds reached 70 km h^{-1}, with gusts of over 120 km h^{-1} recorded at Montague Island..

3.5 2nd April 2008

Peak temperatures along the Gippsland coast coincided with peak wind speeds from the north to north-northwest of 50 km h^{-1}, gusting to 75 km h^{-1}. Temperatures at Bairnsdale, Latrobe Valley and Mt Nowa Nowa were 2-4 ^{o}C warmer than average. Complementary reductions in relative humidity were also observed at these lee stations. The warming and drying along the coast in the lee of the ranges was in contrast to conditions on the upwind side, as can be seen in table 2.

3.6 28th April 2008

Prevailing winds were predominantly westerly and the hottest and driest parts of southeastern Australia were situated along the coastal region of southern New South Wales, in the lee of the main range and coastal escarpment. Interpolated dew point temperature indicated the presence of an extended region of dry air over the Australian Alps, extending into their lee across southern New South Wales. Temperature on the upwind side of the mountains peaked at about 8 ^{o}C below average, while in the lee temperature peaked at only about 1-2 ^{o}C below average, thus indicating a positive anomaly of about 6-7 ^{o}C (see table 2). The elevated temperatures coincided with lower relative humidity and dew point temperature when compared to observations at upwind stations.

3.7 19th September 2008

On evening the 18th of September 2008, with prevailing northwesterly to northeasterly winds, temperatures at Mt Nowa Nowa and Bairnsdale were observed to rise after sunset. Relative humidity at the two coastal stations exhibited complementary behaviour during the night-time period. During the 19th of September, the relatively warm and dry conditions persisted along the Gippsland coast, in contrast to upwind conditions (see table 2).

Observations of temperature, relative humidity and dew point at Moruya also exhibited anomalous maxima and minima during the 19th of September. In figure 13 the temperature trace displays three significant maxima during the 19th, with complementary minima in relative humidity and dew point. These features coincide with brief instances of strong winds from between northwest and north. It is of interest to point out that these foehn-like conditions observed at Moruya were localised; similar maxima and minima were not apparent in the observations recorded at Merimbula where the surface winds remained between northeast and east.

Meso-LAPS output again confirmed the existence of topographically induced, vertically propagating gravity waves at a time when the foehn-like conditions were recorded over the Gippsland coast. Vertical cross-sections of the ω-field, potential temperature isentropes and projected wind vector, which exhibit definite buoyancy wave structure, can be seen in figure 14. The mixing ratio isopleths (not shown) again suggested that foehn-like conditions were associated with partial blocking of moist lower-level air on the windward side of the mountains, with drier air flowing downslope in the lee to replace it.

3.8 20th September 2008

At midday on the 20th of September 2008 the south coast of New South Wales experienced a change in wind direction from between northeast and east to between west and northwest, with an associated increase in wind speed gusting to over 60 km h^{-1}.

Coincident with the wind change, temperatures exhibited an abrupt increase of approximately 8-12 ^{o}C in an hour. By contrast, the temperatures on the upwind side of the mountains only increased by about 2 ^{o}C. Complementary decreases in dew point temperatures of the order of 15-21 ^{o}C in an hour were also observed, with relative humidity falling from around 80% to 8% in an hour. Relative humidity at upwind stations, while falling around 20%, did not match the extreme lows recorded at the lee stations; nor did it match the sharpness of the decline. Approximate regional conditions during the foehn-like event are given in table 2, while the evolution of the event at Moruya can be seen in figure 13.

4. Discussion and Conclusions

The analyses presented above confirm the existence of anomalously warm, dry and windy conditions in the lee of the Australian Alps consistent with foehn occurrence. The observational analyses indicated that the warm and dry conditions experienced in the lee of the ranges cannot be explained by the movement of warm, dry inland air alone. The foehn occurrences considered were shown to result in the regional elevation of fire danger levels over the Gippsland region of Victoria, the region east of the Blue Mountains in New South Wales and the region between the mountains and the southern New South Wales coast. Within this latter region, the coastal escarpment of southern New South Wales was particularly susceptible to elevated fire danger levels due to foehn occurrence.

Numerical analyses using meso-LAPS suggested that foehn occurrence over the regions listed above was primarily connected with partial blocking of relatively moist low-level air on the upwind side of the mountains and subsidence of drier upper-level air in their lee. This implies that the southeastern Australian foehn is primarily of the mechanically-driven type discussed in the introduction. However, our analyses could not completely discount the thermodynamically-driven mechanism. Indeed, after 15:00 AEST on the 27th of May 2007 significant rainfall was recorded at the alpine sites of Mt Hotham, Mt Buller and Falls Creek, all immediately upwind of where the warming and drying occurred. It is therefore possible that alpine rainfall contributed to the drying of the air downwind and that latent heat effects contributed to its warming. Moreover, the 'Lone Pine' fire, which burnt vigorously on east-facing slopes in the southern ACT during May 2005 (refs ????), produced a convection column that displayed a distinct downslope flow while rain was recorded 10 km to the west.

The numerical analyses also consistently revealed the presence of topographically-induced atmospheric waves in connection with foehn occurrence. These waves originated with the descent of upper-level air above or slightly upstream of the ridge top and extended into the lee of the ranges as a broad-scale, vertically propagating gravity wave. Smaller-scale trapped lee mountain waves were also associated with foehn occurrence, as can be seen, for example, in figure 15, which depicts the situation over the southern New South Wales coast at 13:30 AEST on the 27th of October 2008. It is important to note that the manifestation of foehn conditions at the surface is contingent on the interaction of these mountain waves with other atmospheric structures such as inversions. Conditions on the coastal escarpment of southern New South Wales on the 19th of September 2008 are a case in point. On this day foehn-like conditions were intermittently experienced at Moruya (figure13) but not at other nearby stations such at Merimbula. Even though Merimbula may well have been in the lee of the topography, it may have been protected from the downward-propagating dry air by a shallow marine inversion, assisted by the lee trough in the surface pressure field. Hence, the absence of foehn conditions in the surface observations at a particular station doesn't mean that the mountain wave cannot reach the surface somewhere in the surrounding area. The presence of wave structures in model fields and satellite imagery, over regions in southeastern Australia prone to foehn occurrence, should be taken as an indication that foehn conditions are likely, at least somewhere in the region.

The wave structures associated with foehn occurrence mean that they are also an important consideration outside the context of fire weather. They have impacted international sporting events and other pursuits such as light and recreational aviation, e.g. in 2007 a light aircraft crashed north of Melbourne but south of ranges, in severe winds over a region prone to mountain wind waves.

The physical mechanism for foehn occurrence revealed in the analyses also suggests that foehn occurrence is likely in other parts of Australia. Particular examples would include the region to the east of the Flinders Ranges, the region to the east of the ranges in southeast Queensland, Western Australia??? and the eastern part of Tasmania. Indeed, in light of the analyses presented above the claims of Marsh (1987), concerning the contribution of foehn-like flows to the extreme fire weather experienced around Hobart on the 6th of November 1982, appear to be well founded.

Foehn occurrence over southeastern Australia has significant implications for bushfire risk management. The 2nd of April 2008, in particular, was identified by Victorian bushfire authorities as a day of dangerous fire weather in the Gippsland region (G. McCarthy, personal communication). The elevated temperatures and depressed humidity levels associated with foehn winds can result in the accelerated drying-out of wildland fuels, which when coupled with strong winds can increase the severity of fire behaviour characteristics such as flame height, rate of spread and spotting distance (Byram, 1959; Noble et al.,. 1980). As such, foehn occurrence can seriously compromise the safety of fire-fighters and the likely success of fire suppression tactics. For example, the 'Lone Pine' fire in the ACT burnt as a crown fire at night under the influence of foehn-like winds. In this context, it is interesting to note that current bushfire risk management frameworks do not formally account for foehn winds as drivers of bushfire risk, and the likely effects of foehn winds are not generally allowed for in alternate or 'worst case' scenarios.

The seasonality of the foehn events analysed above also has bearing on prescribed burning and hazard reduction strategies. In southeastern Australia, the 'fire season' typically extends from the start of October through to the end of March. Fire managers usually aim to undertake hazard reduction burning just before and after this period, when fire weather conditions are mild, but not so mild that fire in the landscape is unsustainable. Thus, with the exception of the 29th May 2007 event, all of the events analysed fall into the period when prescribed fire is used to reduce wildland fuel loads. Effective bushfire risk management, particularly surrounding prescribed burns, in regions prone to foehn occurrence therefore requires a proper appreciation of the precursor conditions for foehn winds and their likely (spatiotemporal) effect on fire danger levels. In particular, prescribed fires that have not been sufficiently extinguished have significant potential to flare up and become problematic if impacted by foehn conditions. The longer it takes to extinguish a fire the greater the chance of it being impacted by foehn winds.

The foehn events analysed above provide some guidance on synoptic precursors for foehn occurrence in southeastern Australia. The foehn events analysed above all occurred in connection with the passage of low pressure cells through the Great Australian Bight and Bass Strait, which caused strong winds to align nearly perpendicular to certain parts of the Great Dividing Range. This is consistent with the seasonal nature of the foehn occurrences analysed; the study indicated a preference for late autumn into winter and spring. In this context it is interesting to consider the climate change implications for the frequency and extent of foehn occurrence. Hennessey et al. (2005) found that under projected climate change scenarios, it was likely that increased fire weather risk in spring, summer and autumn would increasingly shift periods suitable for prescribed burning toward winter. This effect combined with the effect that global warming is likely to have on the passage of low pressure cells over southern Australia, could result in foehn winds becoming a dominant influence in southeast Australian fire weather. Given the major bushfire problem encountered in southeastern Australia and the expanding population of this region, this aspect of fire weather, which has not been included in Australian fire weather projections to date, would appear to be worthy of further research.

It is important to note that the analyses presented above have focused on 'deep foehn' occurrence, to use the terminology of Mayr and Armi (2008). Study of the 'shallow' or smaller-scale foehn was not possible given the spatial coverage of the observational network and the resolution of the numerical weather model. However, there is a significant likelihood that these events do occur, affecting fire danger levels on smaller scales than what has been analysed. It is also likely that smaller-scale events may be affected by valleys and other smaller-scale terrain features (Drechsel and Mayr, 2008; Mayr and Armi, 2008). A study of the smaller-scale features of foehn winds in southeastern Australia using dense networks of portable automatic weather stations coupled with sub-1km resolution numerical weather models would be a valuable extension of the work discussed above. However, in lieu of such a study, perhaps the best guidance that can be offered in the context of smaller-scale events is that risk and fire behaviour analysts include their possibility in planning as alternate scenarios.

Acknowledgments
This research was carried out as part of the Bushfire Cooperative Research Centre's project B6.3: Managing the risk of bushfire in high-country landscapes. The support of the Bushfire CRC is acknowledged. The authors are also indebted to John Taylor and David Lowe from the School of Physical, Environmental and Mathematical Sciences, University of New South Wales at the Australian Defence Force Academy for taking the time to read earlier drafts of the paper and for their insightful comments. The authors are also grateful to Tony Bannister and Philip Riley of the Bureau of Meteorology and Greg McCarthy of the School of Forest and Ecosystem Science, University of Melbourne for their input and interest in the topic of the paper.

References

Barry, R.G. (1992) *Mountain weather and climate*. 2nd edition. Routledge, New York.

Beck, J.A. (1995) Equations for the forest fire behaviour tables for Western Australia. *CALM Science*, **1**(3), 325-348.

Beer, T. (1974) *Atmospheric waves*. John Wiley & Sons, New York.

Bond et al. (1968) ???????

Brinkmann, W.A.R. (1970) The chinook at Calgary (Canada). *Theoretical and Applied Climatology*, **18**, 269-278.

Brinkmann, W.A.R. (1971) What is a foehn? *Weather*, **26**, 230-239.

Brinkmann, W.A.R (1973) *A climatological study of strong downslope winds in the Boulder area*. NCAR Cooperative Thesis No. 27/INSTARR Occasional Paper No. 7, University of Colrado, 229 pp.

Brinkmann, W.A.R. (1974) Strong downslope winds at Boulder, Colorado. *Monthly Weather Review*, **102**, 592-602.

Byram, G.M. (1959) Forest fire behaviour. In *Forest Fire: Control and Use*, Ed. Davis, K.P. McGraw-Hill, New York.

Carrega, P. (1991) A meteorological index for forest fire hazard in Mediterranean France. *International Journal of Wildland Fire*, **1**(2), 79-86.

Chandler, C., Cheney, P., Thomas, P., Trabaud, L., Williams, D. (1983) *Fire in Forestry, Volume I: Forest Fire Behaviour and Effects*. John Wiley and Sons, NewYork.

Cheney, P., Gould, J., McCaw, L. (2001) The dead-man zone: a neglected area of fire fighter safety. *Australian Forestry*, **64**, 45-50.

Conedera, M., Marxer, P., Hoffmann, C., Tinner, W., Amman, B. (1996). Forest fire research in Switzerland. Part 1: Fire ecology and history research in the Southern part of Switzerland. *International Forest Fire News*, **15**, 13-21.

Conedera, M., Marxer, P., Ambrosetti, P., Della Bruna, G., Spinedi, F. (1998) The 1997 forest fire season in Switzerland. *International Forest Fire News*, **18**, 85-88.

Cook, A.W., Topil, A.G. (1952) Some examples of chinooks east of the mountains in Colorado. *Bulletin of the American Meteorological Society*, **33**(2), 42-47.

Drechsel, S., Mayr, G.J. (2008) Objective forecasting of foehn winds for a subgrid-scale alpine valley. *Weather and Forecasting*, **23**, 205-218.

Drobinski, P., Steinacker, R., Richner, H., Baumann-Stanzer, K., Beffrey, G., Benech, B., Berger, H., Chimani, B., Dabas, A., Dorninger, M., Dürr, B., Flamant, C., Frioud, M., Furger, M., Gröhn, I., Gubser, S., Gutermann, T., Häberli, C., Häller-Scharnhost, E., Jaubert, G., Lothon, M., Mitev, V., Pechinger, U., Piringer, M., Ratheiser, M., Ruffieux, D., Seiz, G., Spatzierer, M., Tschannett, S., Vogt, S., Werner, R., Zängl, G. (2007) Föhn in the Rhine Valley during MAP: A review of its multiscale dynamics in complex valley geometry. *Quarterly Journal of the Royal Meteorological Society*, **133**, 897-916.

Forestry Canada Fire Danger Group (1992) *Development and structure of the Canadian forest fire behaviour prediction system*. Forestry Canada, Science and Sustainable Development Directorate, ST-X-3, Ottawa, Canada.

Frey, K. (1957) Zur diagnose des foehns. *Meteorologische Rundschau*, **10**(6), 181-185.

Gill, A.M., Christian, K.R., Moore, P.H.R., Forrester, R.I. (1987) Bushfire incidence, fire hazard and fuel reduction burning. *Australian Journal of Ecology*, **12**, 299-306.

Gohm, A., Zängl, G., Mayr, G.J. (2004) South foehn in the Wipp Valley on 24 October 1999 (MAP IOP 10): verification of high-resolution numerical simulations with observations. *Monthly Weather Review*, **132**, 78-102.

Gosai, A., Salinger, J. (2003) *Seasonal Fire Weather Outlook March – May 2003*. NIWA Client Report AKL2003-028, National Institute of Water and Atmospheric Research, Auckland.

Gosai, A., Salinger, J. (2004) *Seasonal Fire Weather Outlook March – May 2004*. NIWA Client Report AKL2004-20, National Institute of Water and Atmospheric Research, Auckland.

Gosai, A., Salinger, J. (2005) *Seasonal Fire Weather Outlook March – May 2005*. NIWA Client Report AKL2005-018, National Institute of Water and Atmospheric Research, Auckland.

Hann, J. (1866) Zur Frage über den Ursprung des Föhn. *Zeitschrift der österreichischen Gesellschaft für Meteorologie*, **1**(1), 257-263.

Hann, J. (1867) Der Föhn in den österreichischen Alpen. *Zeitschrift der österreichischen Gesellschaft für Meteorologie*, **2**(19), 433-445.

Hennessey, K., Lucas, C., Nicholls, N., Bathols, J., Suppiah, R., Ricketts, J. (2005) *Climate change impacts on fire-weather in south-east Australia*. Commonwealth Scientific and Industrial Research Organisation, Canberra, ACT.

Hoinka, K.P. (1985) Observation of airflow over the Alps during a foehn event. *Quarterly Journal of the Royal Meteorological Society*, **111**, 199-224.

Huang, X, Mills, G.A. (2006) *Objective identification of wind change timing from single station observations*. BMRC Research Report No 120. 88pp.

Huschke, R.E. (1959) *Glossary of Meteorology*. American Meteorological Society, Boston.

Keeley, J.E. (2004) Impact of antecedent climate on fire regimes in coastal California. *International Journal of Wildland Fire*, **13**(2), 173-182.

Kondo, J., Kuwagata, T. (1992) Enhancement of forest fires over northeastern Japan due to atypical strong dry wind. *Journal of Applied Meteorology*, **31**, 386-396.

Lim, J-H. (2002) Fire situation in Republic of Korea. *International Forest Fire News*, **26**, 61-65.

Lockwood, J.G. (1962) Occurrence of föhn winds in the British Isles. *The Meteorological Magazine*, **91**, 57-65.

Marsh, L. (1987) *Fire weather forecasting in Tasmania*. Meteorological Note 171. Bureau of Meteorology, Australia.

Mayr, G.J., Armi, L. (2008) Föhn as a response to changing upstream and downstream air masses. *Quarterly Journal of the Royal Meteorological Society*, **134**, 1357-1369.

McArthur, A.G. (1966) Weather and grassland fire behaviour. Department of National Development, Forestry and Timber Bureau Leaflet No. 100. Canberra, Australia.

McArthur, A.G. (1967) Fire behaviour in eucalypt forests. Department of National Development, Forestry and Timber Bureau Leaflet No. 107. Canberra, Australia.

McGowan, H.A., Sturman, A.P. (1996) Regional and local scale characteristics of fohn wind events over the South Island of New Zealand. *Meteorology and Atmospheric Physics*, **58,** 151-164.

Mills, G.A. (2002) A case of coastal interaction with a cool change. *Australian Meteorological Magazine*, **51**, 203-221.

Mills, G.A. (2005) A re-examination of the synoptic and mesoscale meteorology of Ash Wednesday 1983. *Australian Meteorological Magazine*, **54**, 35-55.

Mills, G.A., (2007) On easterly changes over elevated terrain in Australia's southeast. *Australian Meteorological Magazine*, **56**, 177-190.

Mills, G.A., Pendlebury, S. (2003) Processes leading to a severe wind-shear incident at Hobart Airport. *Australian Meteorological Magazine*, **52**, 171-188.

Ninomiya, K., Yamagishi, Y., Ohno, H., Miura, N. (1985). Analysis and numerical prediction experiment of extremely strong dry wind occurred over the northeastern Japan on 27 April 1983. *Journal of the Meteorological Society of Japan*, **63**, 589-604.

Noble, I.R., Bary, G.A.V, Gill, A.M. (1980) McArthur's fire-danger meters expressed as equations. *Australian Journal of Ecology*, **5**, 201-203.

Osmond, H.L. (1941) The chinook wind east of the Canadian Rockies. *Canadian Journal of Research A*, **19**(4), 57-66.

Puri, K., Dietachmayer, G.D., Mills, G.A., Davidson, N.E., Bowen, R.A., Logan, L.W. (1998) The new BMRC Limited Area prediction System, LAPS. *Australian Meteorological Magazine*, **47**, 203-223.

Rothermel, R.C. (1972) *A mathematical model for predicting fire spread in wildland fuels*. USDA Forest Service, Intermountain Research Station, INT-115, Ogden, Utah, USA.

Salinger, J., Porteous, A., Renwick, J. (2000) *Seasonal Fire Weather Outlook September – November 2000.* NIWA Report AK00102, National Institute of Water and Atmospheric Research, Auckland.

Salinger, J., Porteous, A. (2002) *Seasonal Fire Weather Outlook January - March 2002*. NIWA Report AK02003, National Institute of Water and Atmospheric Research, Auckland.

Seibert, P. (1990) South foehn studies since the ALPEX experiment. *Meteorology and Atmospheric Physics*, **43**, 91-103.

Sharples, J.J. (2009) Review of mountain meteorological effects relevant to fire behaviour and bushfire risk. *International Journal of Wildland Fire* (in press).

Sneeuwjagt, R.J., Peet, G.B. (1985) *Forest fire behaviour tables for Western Australia*, 3rd Edn Department of Conservation and Land Management, Perth, Western Australia.

Ustrnul, Z. (1992) Influence of foehn winds on air temperature and humidity in the Polish Carpathians. *Theoretical and Applied Climatology*, **45**(1), 43-47.

Van Wagner, C.E., Pickett, T.L. (1985) Equations and FORTRAN program for the Canadian Forest Fire Weather Index System. *Environment Canada, Forestry Service*, **33**, Ottawa, Canada.

Vergeiner, I. (1971) Comments on: The Chinook at Calgary (Canada) by Waltraud A. R. Brinkmann. *Theoretical and Applied Climatology*, **19**, 339-341.

Whiteman, C.D. (2000) *Mountain meteorology fundamentals and applications*. Oxford University Press, New York.

WMO. (1992) *International Meteorological Vocabulary*. 2nd Edition. Volume 182. World Meteorological Organization.

Table and figure captions:

Table 1. Bureau of Meteorology station number, station name, longitude, latitude and elevation for stations considered in the study. Mean maximum monthly temperatures for each of the stations are listed. Mean monthly maximum temperature data was unavailable for stations marked with an asterisk. Approximate values are listed, as derived from a nearby station.

Table 2. A comparison of downwind and upwind conditions for the foehn-like events discussed in sections 3.3 – 3.8. The approximate characteristic temperatures, relative humidity and dew point temperatures for each of the events are listed.

Figure 1. Visual band satellite image of southeast Australia taken at 02:33 UTC, 29th May 2007. The image shows cloud features consistent with foehn occurrence over southeastern Australia.

Figure 2. (a) Map of southeastern Australia showing the locations of the automatic weather stations used in the study and the topography of the Australian Alps, (b) Map of topography and automatic weather stations in the Blue Mountains region.

Figure 3. Topographic contours (200m spacing) of 10 km resolution digital elevation model overlayed with surfaces of (a) air temperature (^{o}C), (b) relative humidity (%), (c) dew point temperature (^{o}C) and (d) McArthur mark 5 Forest Fire Danger Rating (FFDR), interpolated from Bureau of Meteorology data for 15:00 AEST, 29th May 2007. The arrow in panel (a) indicates the approximate direction of the upper winds.

Figure 4. Time series of (a) Temperature, (b) Relative Humidity and (c) Dew point for East Sale, Melbourne and Wangaratta for the period 28th May – 31st May 2007 (AEST).

Figure 5. Two-hourly meso-LAPS output of 500 hPa level ω-field for 22:00 UTC, 28th May 2007 – 08:00 UTC, 29th May 2007 (08:00 – 18:00 AEST, 29th May 2007). Red contours indicate positive ω values (descending air) and black contours indicate negative ω values (ascending air). The grey shading represents the elevation of smoothed topography in metres. The dashed line in the top left panel is the cross section used in figure 8.

Figure 6. Meso-LAPS output for 23:00 UTC, 28th May 2007 (07:00 AEST, 29th May 2007) showing vertical cross-sections of (a) ω-isopleths (units????*****)with positive values indicated by solid lines, negative values dashed, (b) mixing ratio isopleths (g kg^{-1}), (c) potential temperature isentropes (K) in red and projected wind vector. The cross section is shown in plan view in the top left panel of figure 7.

Figure 7. Topographic contours (200m spacing) of 10 km resolution digital elevation model overlayed with surfaces of (a) air temperature (^{o}C), (b) relative humidity (%), (c) dew point temperature (^{o}C) and (d) McArthur mark 5 Forest Fire Danger Rating (FFDR), interpolated from Bureau of Meteorology data for 11:00 AEST, 27th October 2008. The arrow in panel (a) indicates the approximate direction of the upper winds.

Figure 8. Topographic contours (200m spacing) of 10 km resolution digital elevation model overlayed with surfaces of (a) air temperature (^{o}C), (b) relative humidity (%), (c) dew point temperature (^{o}C) and (d) McArthur mark 5 Forest Fire Danger Rating (FFDR), interpolated from Bureau of Meteorology data for 15:00 AEST, 27th October 2008. The arrow in panel (a) indicates the approximate direction of the upper winds.

Figure 9. Time series of (a) Temperature, (b) Relative Humidity and (c) Dew point for Bega, Orbost and Albury for the period 26th October – 29th October 2008 (AEST).

Figure 10. Potential temperature isentropes and low-level wind barbs from 0.125 degree LAPS, for the times 00:00, 03:00, 06:00 and 09:00 UTC, 27th October 2008. The sequence shows the passage of a cold

front that ends the foehn-like event at Orbost (at approx. 01:00 UTC) and then at Bega (at approx. 07:30 UTC).

Figure 11. Time series (12:00 AEST 26th October – 12:00 AEST 28th October 2008) of (a) Wind speed and gust at Orbost, (b) Wind speed and gust at Bega.

Figure 12. Meso-LAPS output for 23:00 UTC, 26th October 2008 (09:00 AEST, 27th October 2008): (a) 500 hPa level ω-field (units????*****); red contours indicate positive ω values (descending air) and black contours indicate negative ω values (ascending air), (b) Vertical cross-section of mixing ratio isopleths (g kg^{-1}), and (c) Vertical cross-section of potential temperature isentropes (K) in red and projected wind vector. The cross-section used in panels (b) and (c) is indicated in panel (a) by the dashed line.

Figure 13. Temperature, relative humidity and dew point time series for Moruya, 18th September – 21st September 2008.

Figure 14. Meso-LAPS output for 21:00 UTC 18th September 2008. (a) Vertical cross-section of ω isopleths (units????*****), (b) Vertical cross-section of potential temperature isentropes (K) and projected wind vector.

Figure 15. Visual satellite image taken at 03:30 UTC 27th October 2008. Lee mountain wave clouds are apparent over southern New South Wales.

Table 1.

AWS ID	AWS Name	Long.	Lat.	Elev. (m)	Mean Maximum Temperature (°C) Jan	Feb	Mar	Apr	May	Jun	Jul	Aug	Sep	Oct	Nov	Dec
070014	Canberra Airport	149.20	-35.30	578.4	27.9	27.1	24.5	20.0	15.5	12.2	11.3	13.0	16.1	19.4	22.6	26.1
070217	Cooma Airport	148.97	-36.29	930.0	26.2	25.2	22.4	18.3	14.2	10.9	10.2	12.2	14.9	18.0	20.8	24.1
070328	Bombala	149.23	-37.00	760.5	25.0	24.0	21.7	17.9	14.3	10.9	10.6	12.4	15.2	17.5	20.1	23.2
072150	Wagga Wagga	147.46	-35.16	212.0	31.5	30.8	27.7	22.5	17.3	13.8	12.6	14.5	17.5	21.3	25.6	29.4
072160	Albury	146.95	-36.07	163.5	31.7	31.0	27.7	22.4	17.7	13.9	13.0	15.1	17.8	21.4	25.5	29.3
081125	Shepparton*	145.39	-36.43	113.9	29.4	29.4	26.3	21.5	17.2	13.9	13.0	14.8	17.3	20.8	24.5	27.4
082138	Wangaratta	146.31	-36.42	152.6	31.6	30.8	27.6	22.5	17.5	13.9	12.9	14.5	17.4	21.0	25.4	29.0
084144	Mt Nowa Nowa	148.09	-37.69	350.0	24.6	24.4	22.4	19.1	15.8	13.5	12.8	14.5	16.9	18.9	20.6	22.2
085279	Bairnsdale	147.57	-37.88	49.4	25.6	25.4	23.7	20.6	17.5	15.0	14.4	15.6	17.4	19.6	21.5	23.5
084145	Orbost*	148.47	-37.69	62.7	25.4	25.4	23.8	20.8	17.7	15.2	14.8	16.0	17.8	19.8	21.5	23.6
086282	Melbourne Airport	144.83	-37.67	113.4	26.2	26.4	24.0	20.2	16.6	13.6	13.0	14.4	16.5	19.1	21.7	24.4
085072	East Sale Airport	147.13	-38.12	4.6	25.4	25.3	23.5	20.3	16.8	14.2	13.7	15.0	16.9	19.2	21.2	23.3
085280	Latrobe Valley	146.47	-38.21	55.7	25.9	26.2	23.2	19.8	16.2	13.6	13.1	14.2	16.1	18.7	21.0	23.8
063292	Mount Boyce	150.27	-33.62	1080.0	23.7	22.6	20.3	17.1	13.6	10.3	9.4	11.2	14.4	17.5	19.5	22.2
063303	Orange Airport	149.13	-33.38	947.4	26.9	25.9	23.1	18.6	14.2	11.1	9.7	11.2	14.8	17.8	21	24.6
067113	Penrith Lakes	150.68	-33.72	24.7	30.5	29.4	27.5	24.6	21	18.3	17.7	19.7	23.1	25.7	26.8	29.3
069017	Montague Island	150.23	-36.25	52.0	22.9	23.3	22.4	20.4	18.2	16.1	15.4	16	17.4	18.7	19.9	21.7
069132	Braidwood	149.78	-35.43	665.2	26.5	25.4	22.8	19.5	15.9	12.6	12	13.5	16.3	18.9	21.3	24.4
069137	Green Cape	150.05	-37.26	19.4	21.6	22.1	21.3	19.7	17.3	15.1	14.4	14.8	15.9	17.3	18.6	20.1
069138	Ulladulla	150.48	-35.36	35.7	24	24.4	23.4	21.5	19	17	16.3	17.3	19	20.8	21.4	22.9
069139	Bega	149.82	-36.67	41.0	26.7	26.4	24.5	22.2	19.2	16.6	16.1	17.7	19.7	21.6	22.9	24.8
069147	Merimbula Airport*	149.9	-36.91	1.5	24.3	24.6	23.4	21.2	18.7	16.3	15.8	16.8	18.3	20	21.2	23
069148	Moruya Airport*	150.14	-35.9	4.0	23.9	24	23.3	21.6	19.1	16.8	16.2	17.1	18.7	20.1	21.4	22.8

Table 2.

Date and Downwind Region	Downwind Conditions			Upwind Conditions		
	Temp (°C)	**RH (%)**	**Dew (°C)**	**Temp (°C)**	**RH (%)**	**Dew (°C)**
29 Sep 2000 NSW Sth Coast	32	20	4	20	55	10
29 Sep 2000 NSW Blue Mtns	35	13	2	21	55	12
1 Oct 2000 NSW Sth Coast	19	15	-8	12	42	3
2 Apr 2008 VIC SE Coast	26	25	3	18	54	8
28 Apr 2008 NSW Sth Coast	18	30	-1	11	57	3
19 Sep 2008 VIC SE Coast	16	31	-1	8	82	9
20 Sep 2008 NSW Sth Coast	30	8	-9	21	27	2

Figure 1.

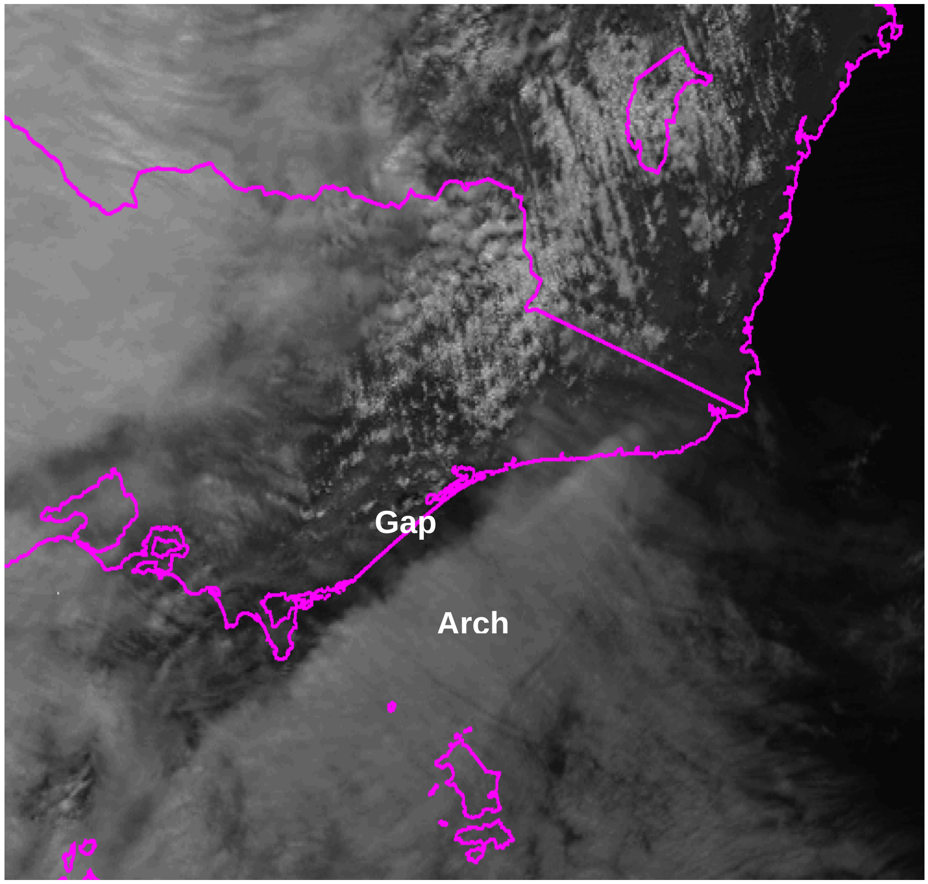

Figure 2

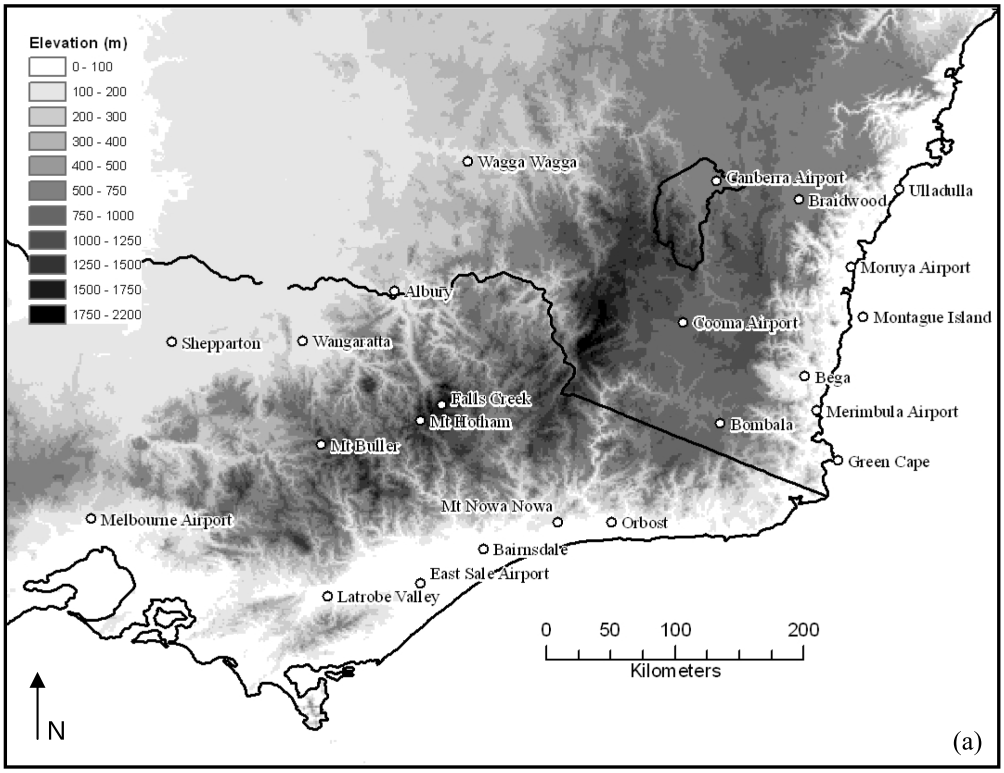

Elevation (m)
0 - 100
100 - 200
200 - 300
300 - 400
400 - 500
500 - 750
750 - 1000
1000 - 1250
1250 - 1500
1500 - 1750
1750 - 2200
Wagga Wagga
Canberra Airport
Braidwood
Ulladulla
Moruya Airport
Albury
Cooma Airport
Montague Island
Shepparton
Wangaratta
Bega
Falls Creek
Mt Hotham
Merimbula Airport
Bombala
Mt Buller
Green Cape
Mt Nowa Nowa
Orbost
Melbourne Airport
Bairnsdale
East Sale Airport
Latrobe Valley
0 50 100 200
Kilometers
N
(a)

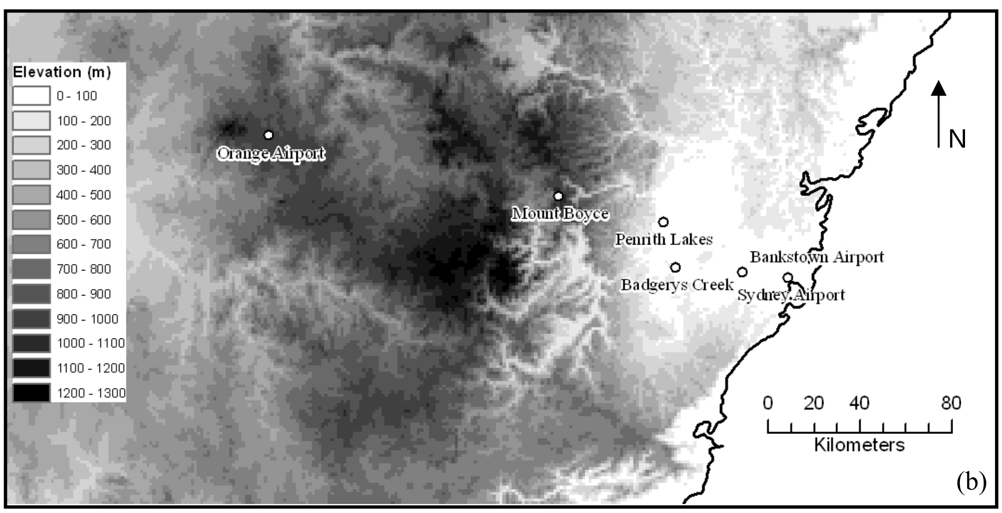

Elevation (m)
0 - 100
100 - 200
200 - 300
300 - 400
400 - 500
500 - 600
600 - 700
700 - 800
800 - 900
900 - 1000
1000 - 1100
1100 - 1200
1200 - 1300
Orange Airport
Mount Boyce
Penrith Lakes
Bankstown Airport
Badgerys Creek
Sydney Airport
N
0 20 40 80
Kilometers
(b)

Figure 3. (29/05/07)

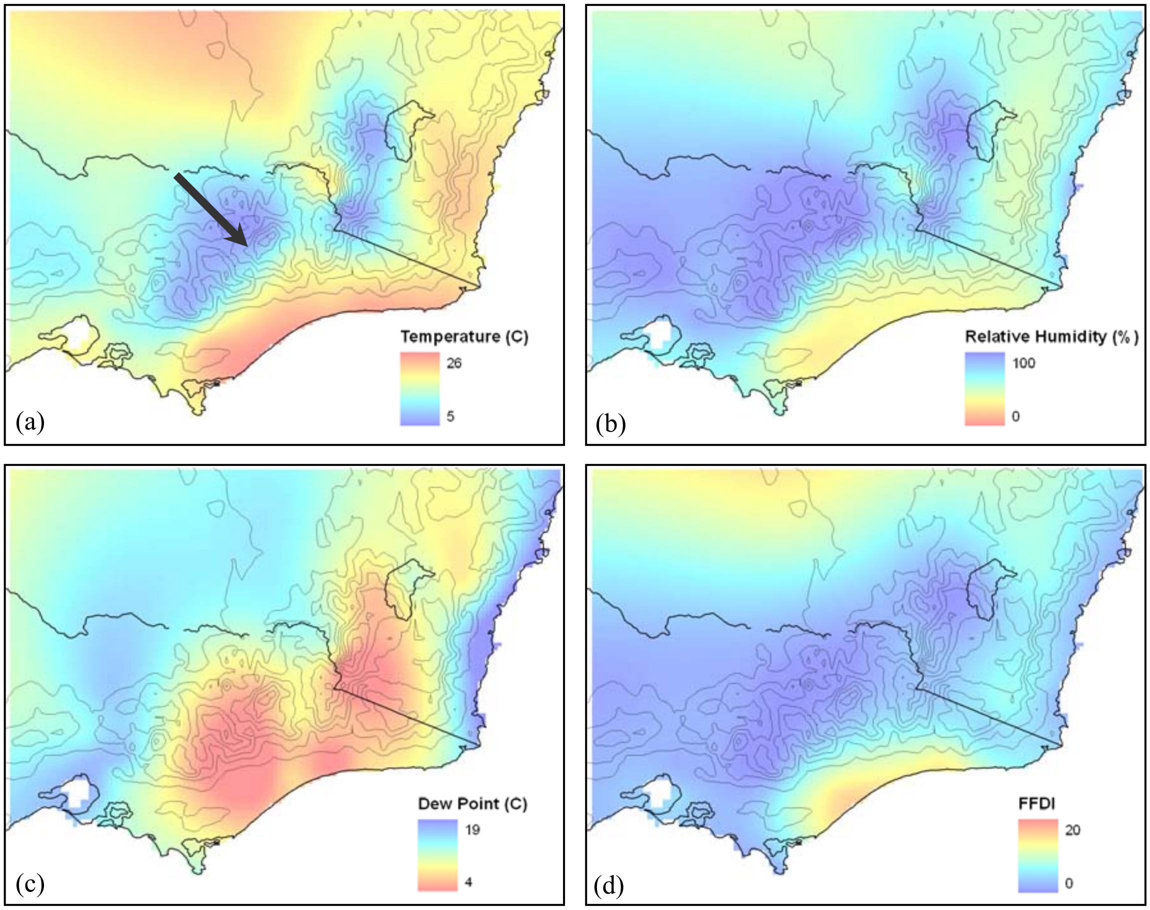

Figure 4.

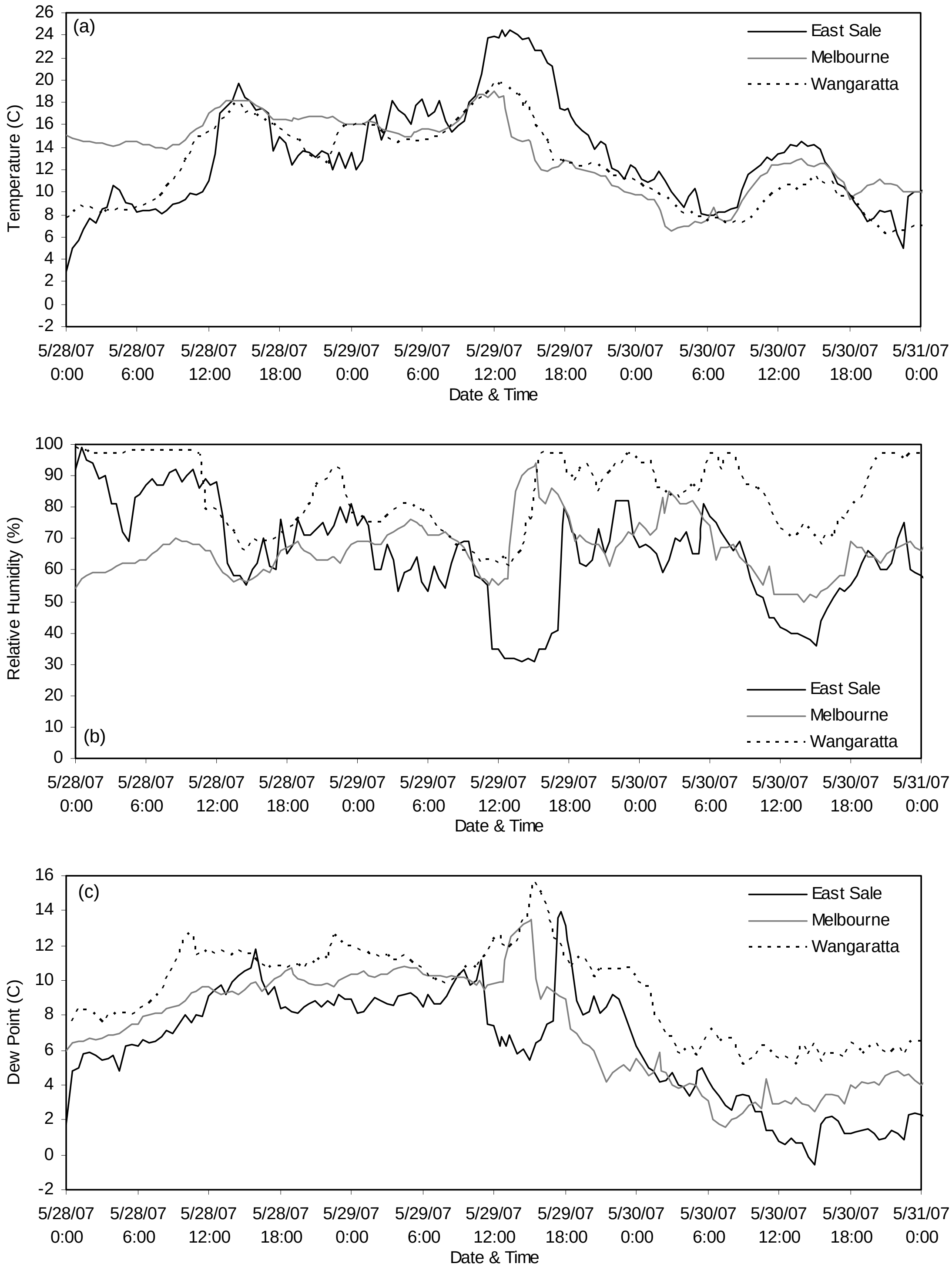

(a)
East Sale
Melbourne
Wangaratta
Temperature (C)
26
24
22
20
18
16
14
12
10
8
6
4
2
0
-2
5/28/07 0:00
5/28/07 6:00
5/28/07 12:00
5/28/07 18:00
5/29/07 0:00
5/29/07 6:00
5/29/07 12:00
5/29/07 18:00
5/30/07 0:00
5/30/07 6:00
5/30/07 12:00
5/30/07 18:00
5/31/07 0:00
Date & Time
Relative Humidity (%)
100
90
80
70
60
50
40
30
20
10
0
(b)
East Sale
Melbourne
Wangaratta
Date & Time
(c)
East Sale
Melbourne
Wangaratta
Dew Point (C)
16
14
12
10
8
6
4
2
0
-2
Date & Time

Figure 5.

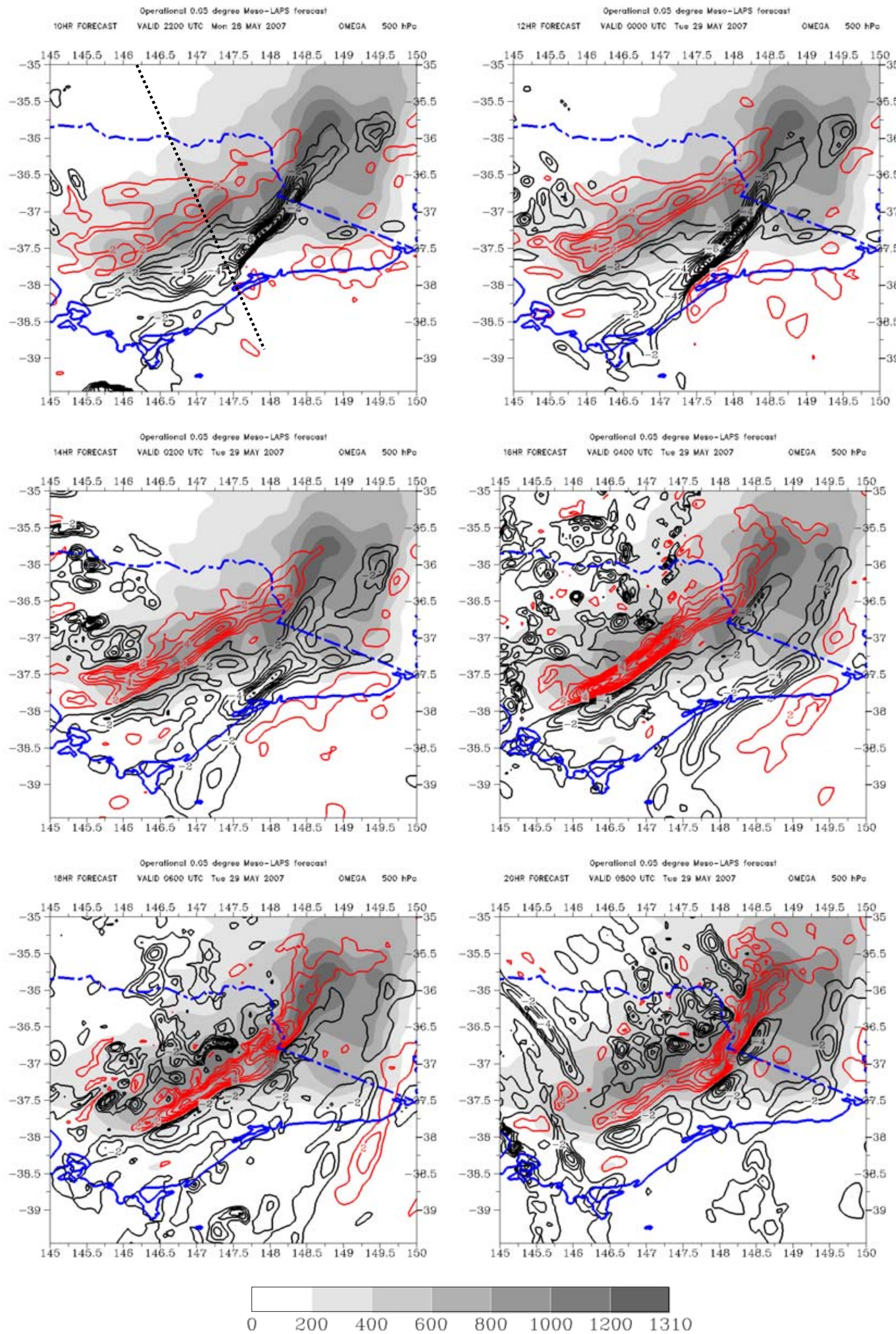

Operational 0.05 degree Meso-LAPS forecast
10HR FORECAST VALID 2200 UTC Mon 28 MAY 2007 OMEGA 500 hPa
Operational 0.05 degree Meso-LAPS forecast
12HR FORECAST VALID 0000 UTC Tue 29 MAY 2007 OMEGA 500 hPa
Operational 0.05 degree Meso-LAPS forecast
14HR FORECAST VALID 0200 UTC Tue 29 MAY 2007 OMEGA 500 hPa
Operational 0.05 degree Meso-LAPS forecast
16HR FORECAST VALID 0400 UTC Tue 29 MAY 2007 OMEGA 500 hPa
Operational 0.05 degree Meso-LAPS forecast
18HR FORECAST VALID 0600 UTC Tue 29 MAY 2007 OMEGA 500 hPa
Operational 0.05 degree Meso-LAPS forecast
20HR FORECAST VALID 0800 UTC Tue 29 MAY 2007 OMEGA 500 hPa
0 200 400 600 800 1000 1200 1310

Figure 6.

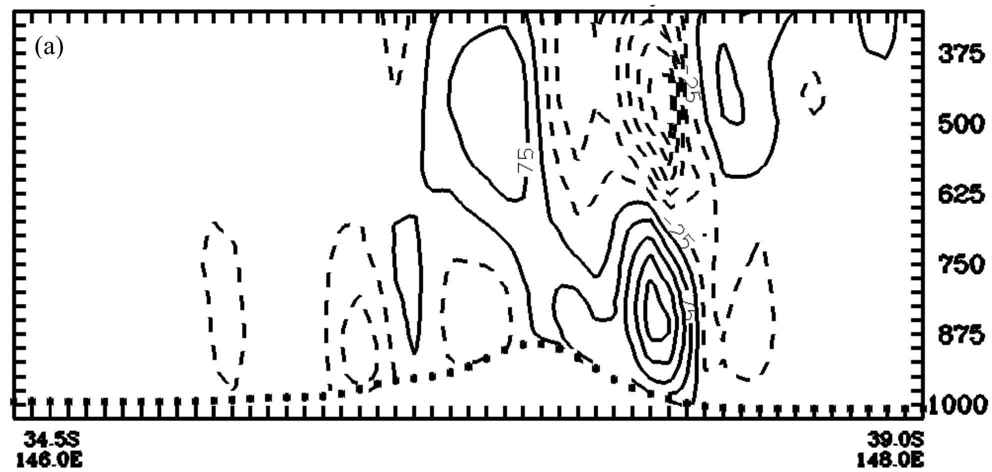
(a)
75
25
25
75
375
500
625
750
875
1000
34.5S
146.0E
39.0S
148.0E

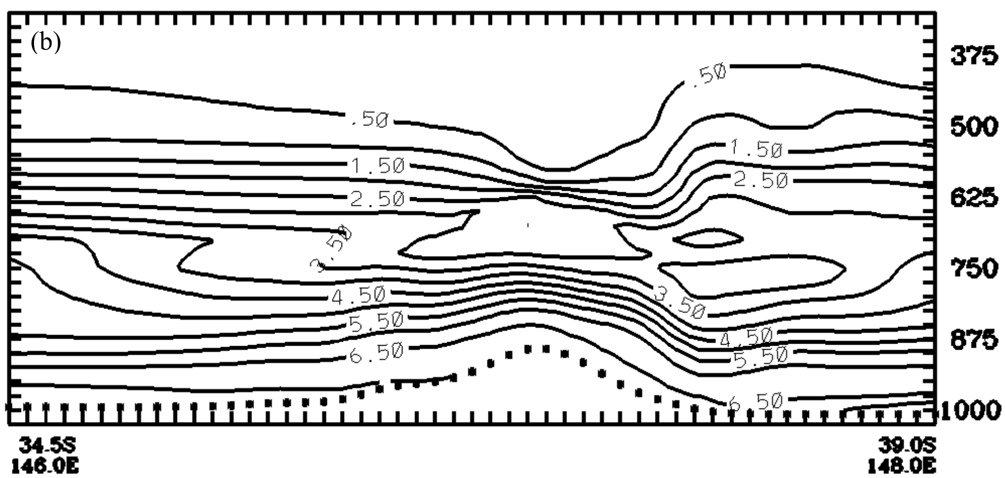
(b)
.50
.50
1.50
1.50
2.50
2.50
3.50
3.50
4.50
4.50
5.50
5.50
6.50
6.50
375
500
625
750
875
1000
34.5S
146.0E
39.0S
148.0E

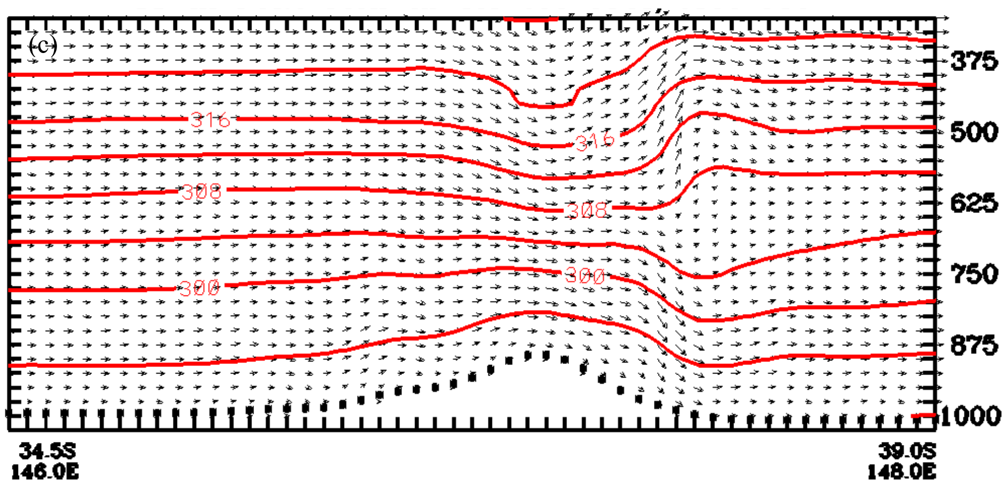
(c)
316
316
308
308
300
300
375
500
625
750
875
1000
34.5S
146.0E
39.0S
148.0E

Figure 7. (27/10/08 11am)

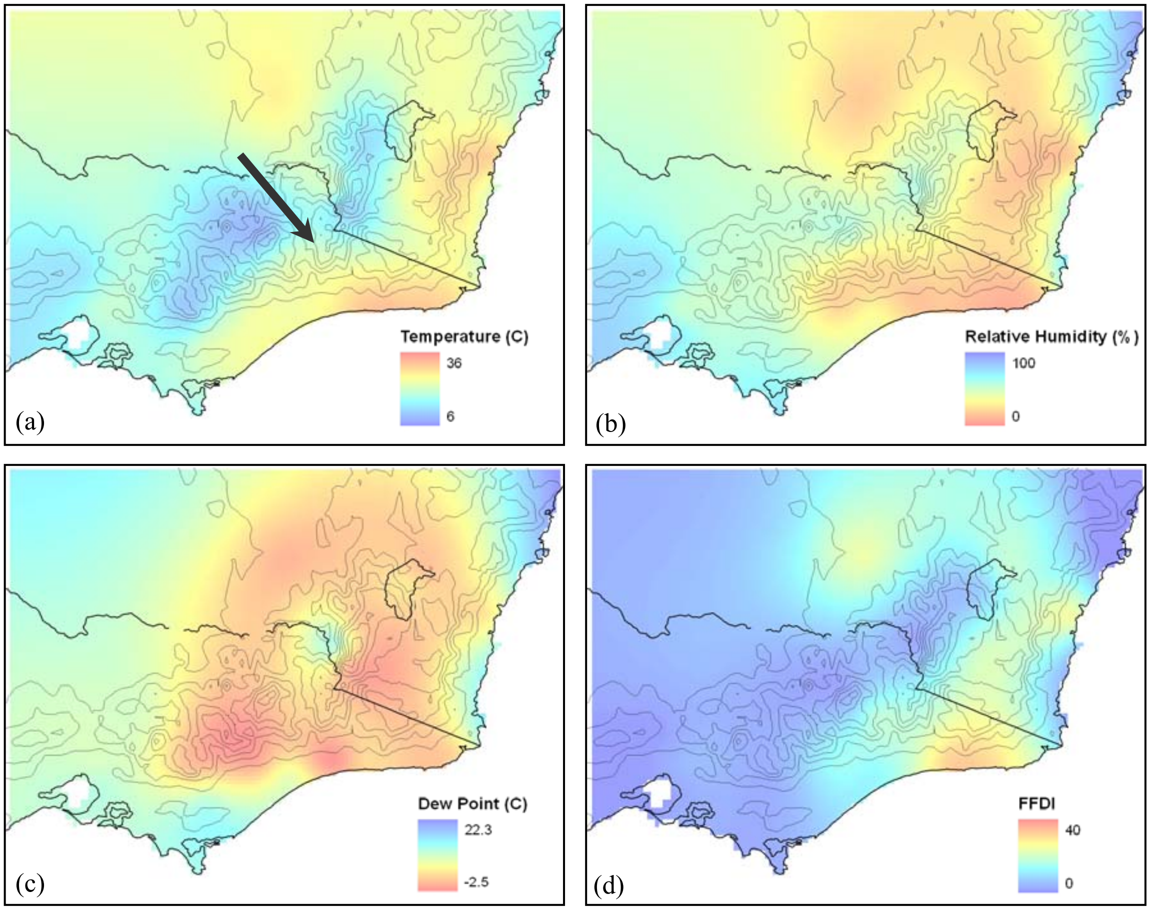

Figure 8. (27/10/08 3pm)

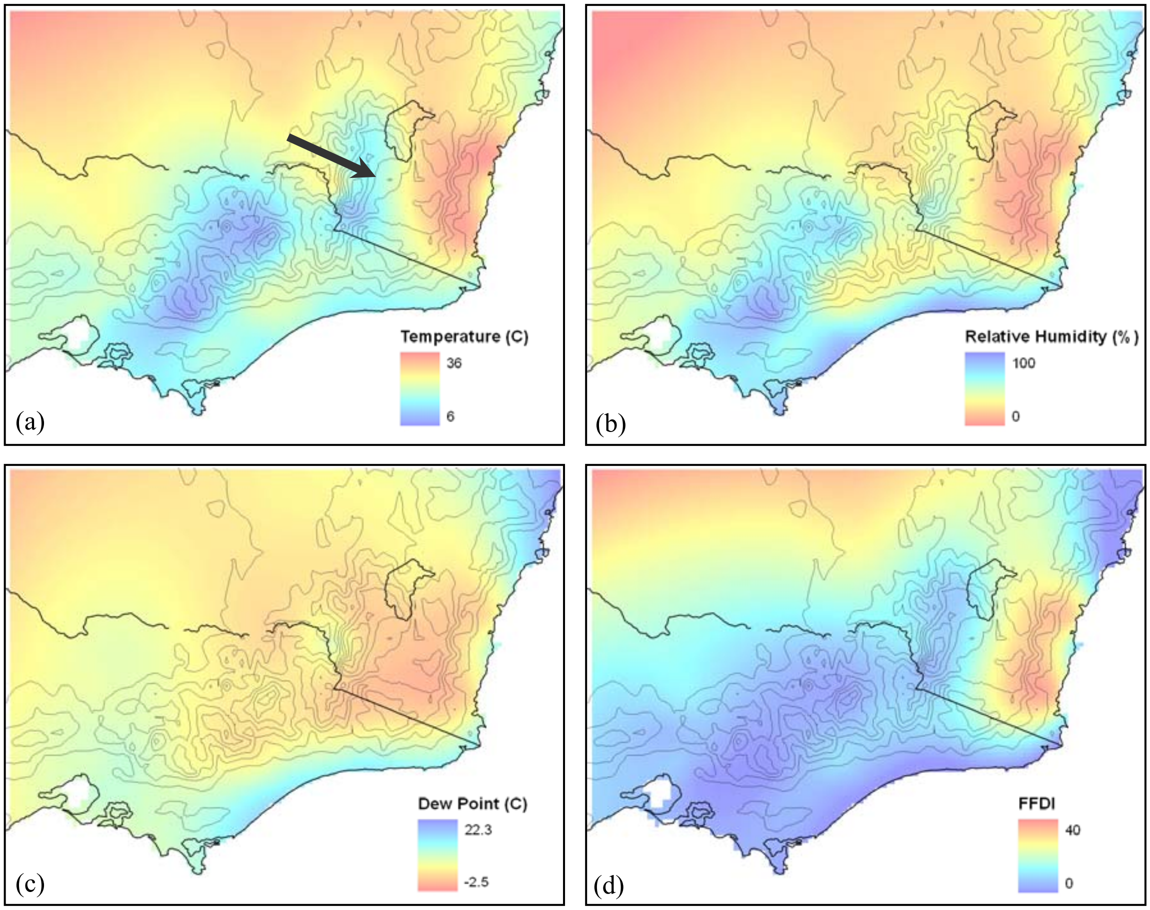

Figure 9.

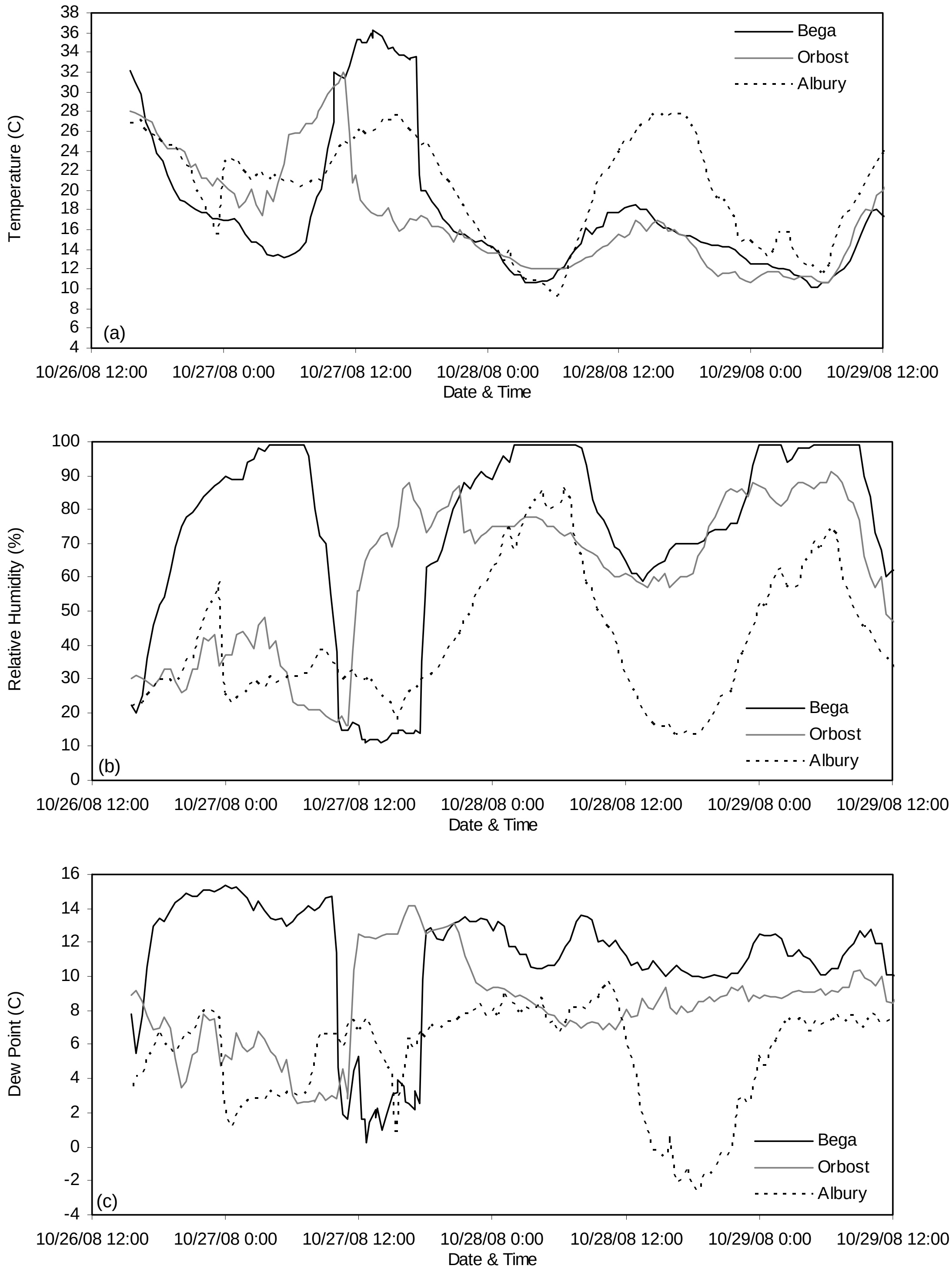

Temperature (C)
Bega
Orbost
Albury
(a)
10/26/08 12:00
10/27/08 0:00
10/27/08 12:00
10/28/08 0:00
10/28/08 12:00
10/29/08 0:00
10/29/08 12:00
Date & Time
Relative Humidity (%)
(b)
Dew Point (C)
(c)

Figure 10.

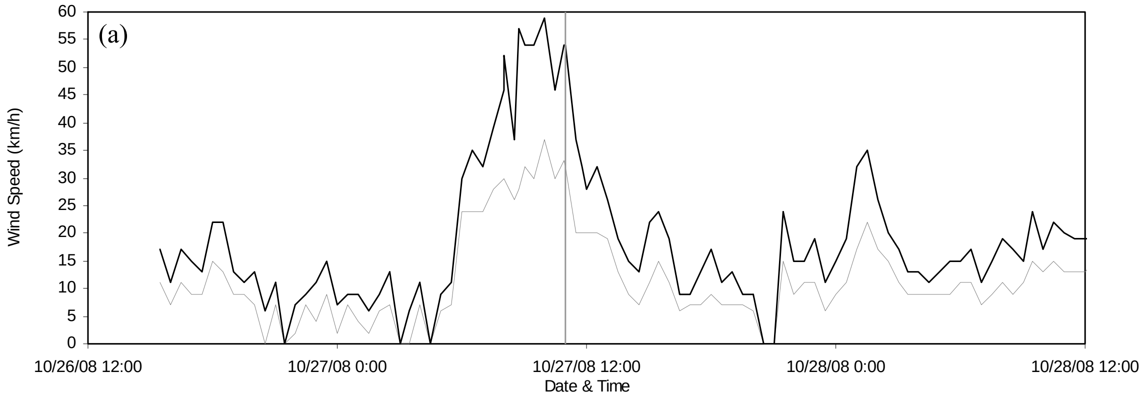
(a)
Wind Speed (km/h)
Date & Time
60
55
50
45
40
35
30
25
20
15
10
5
0
10/26/08 12:00
10/27/08 0:00
10/27/08 12:00
10/28/08 0:00
10/28/08 12:00

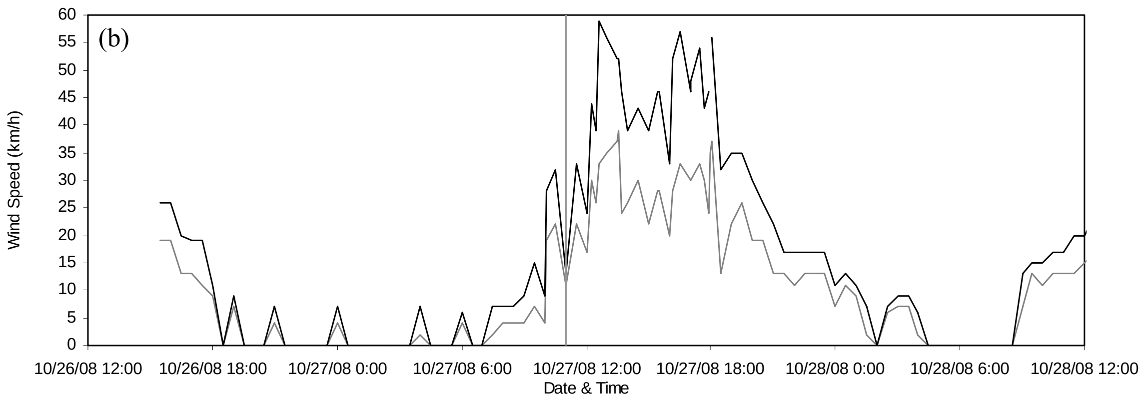
(b)
Wind Speed (km/h)
Date & Time
60
55
50
45
40
35
30
25
20
15
10
5
0
10/26/08 12:00
10/26/08 18:00
10/27/08 0:00
10/27/08 6:00
10/27/08 12:00
10/27/08 18:00
10/28/08 0:00
10/28/08 6:00
10/28/08 12:00

Figure 11

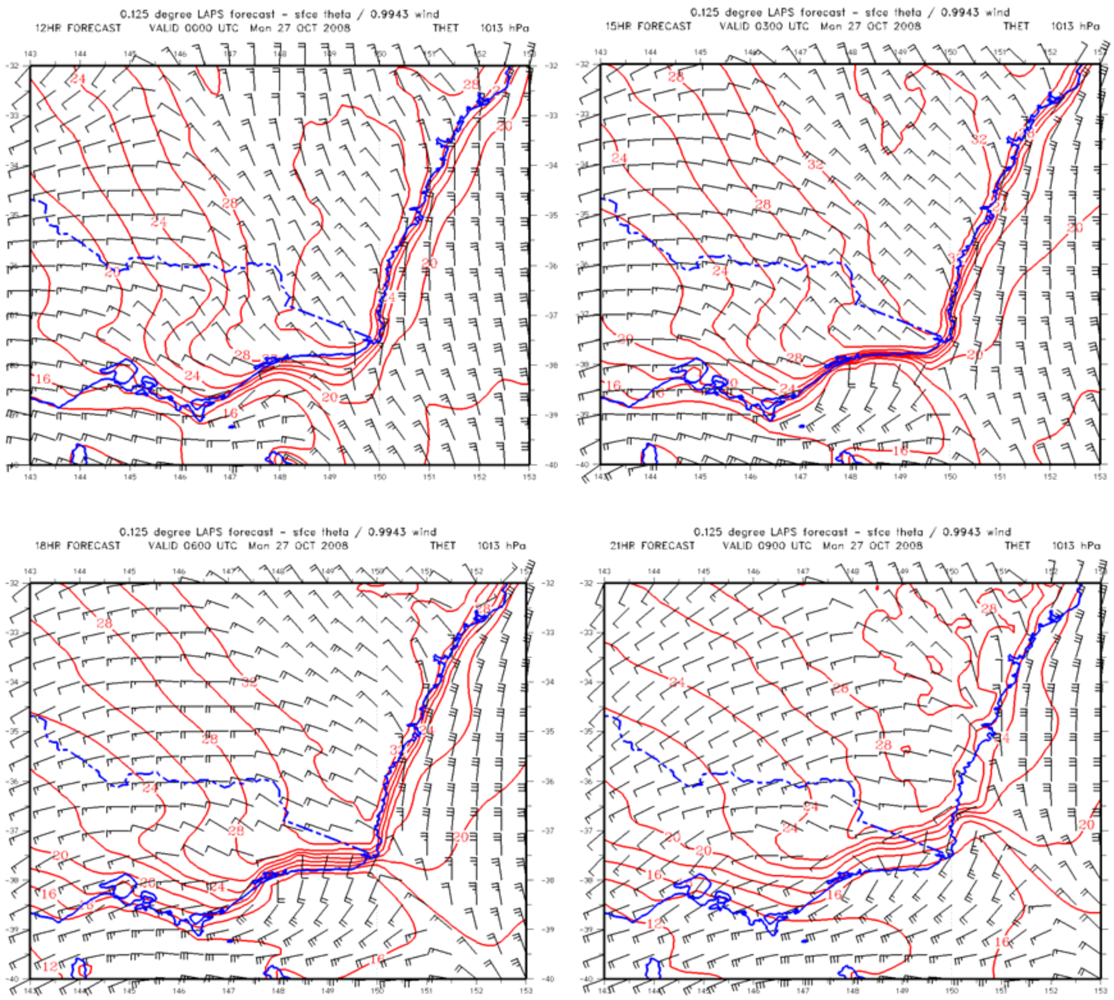
0.125 degree LAPS forecast - sfce theta / 0.9943 wind
12HR FORECAST VALID 0000 UTC Mon 27 OCT 2008 THET 1013 hPa
0.125 degree LAPS forecast - sfce theta / 0.9943 wind
15HR FORECAST VALID 0300 UTC Mon 27 OCT 2008 THET 1013 hPa
0.125 degree LAPS forecast - sfce theta / 0.9943 wind
18HR FORECAST VALID 0600 UTC Mon 27 OCT 2008 THET 1013 hPa
0.125 degree LAPS forecast - sfce theta / 0.9943 wind
21HR FORECAST VALID 0900 UTC Mon 27 OCT 2008 THET 1013 hPa

Figure 12.

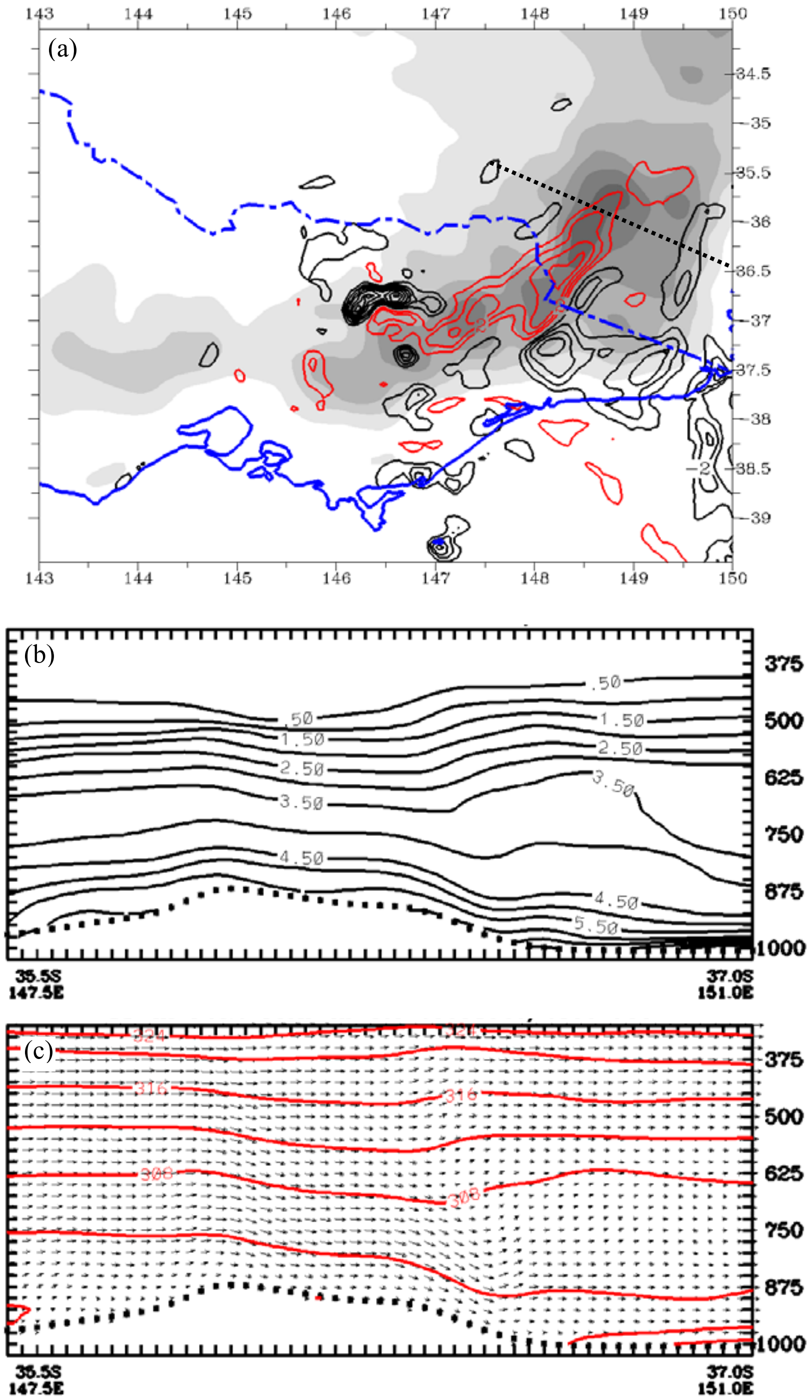

(a)
143
144
145
146
147
148
149
150
-34.5
-35
-35.5
-36
-36.5
-37
-37.5
-38
-38.5
-39
(b)
.50
1.50
2.50
3.50
4.50
5.50
375
500
625
750
875
1000
35.5S 147.5E
37.0S 151.0E
(c)
324
316
300
375
500
625
750
875
1000
35.5S 147.5E
37.0S 151.0E

Figure 13.

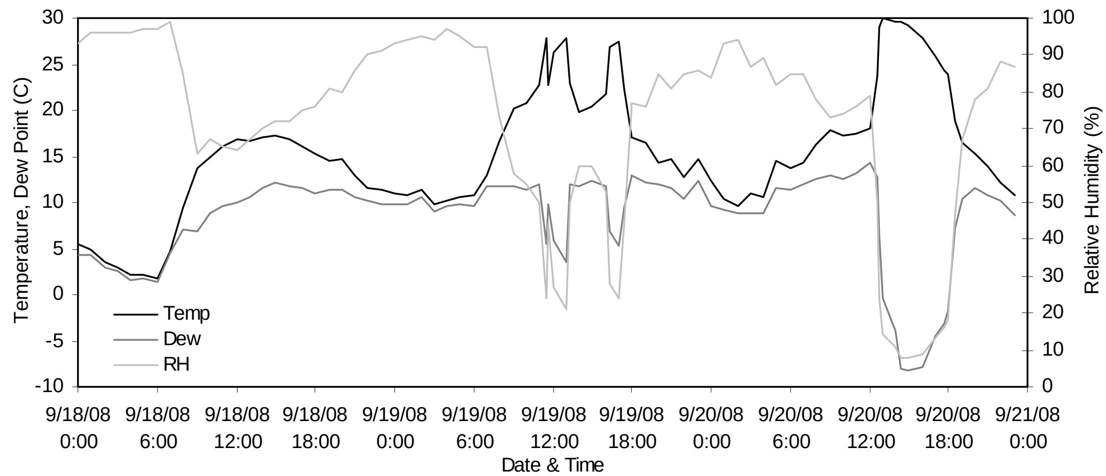

30
25
20
15
10
5
0
-5
-10
Temperature, Dew Point (C)
100
90
80
70
60
50
40
30
20
10
0
Relative Humidity (%)
Temp
Dew
RH
9/18/08 0:00
9/18/08 6:00
9/18/08 12:00
9/18/08 18:00
9/19/08 0:00
9/19/08 6:00
9/19/08 12:00
9/19/08 18:00
9/20/08 0:00
9/20/08 6:00
9/20/08 12:00
9/20/08 18:00
9/21/08 0:00
Date & Time

Figure 14.

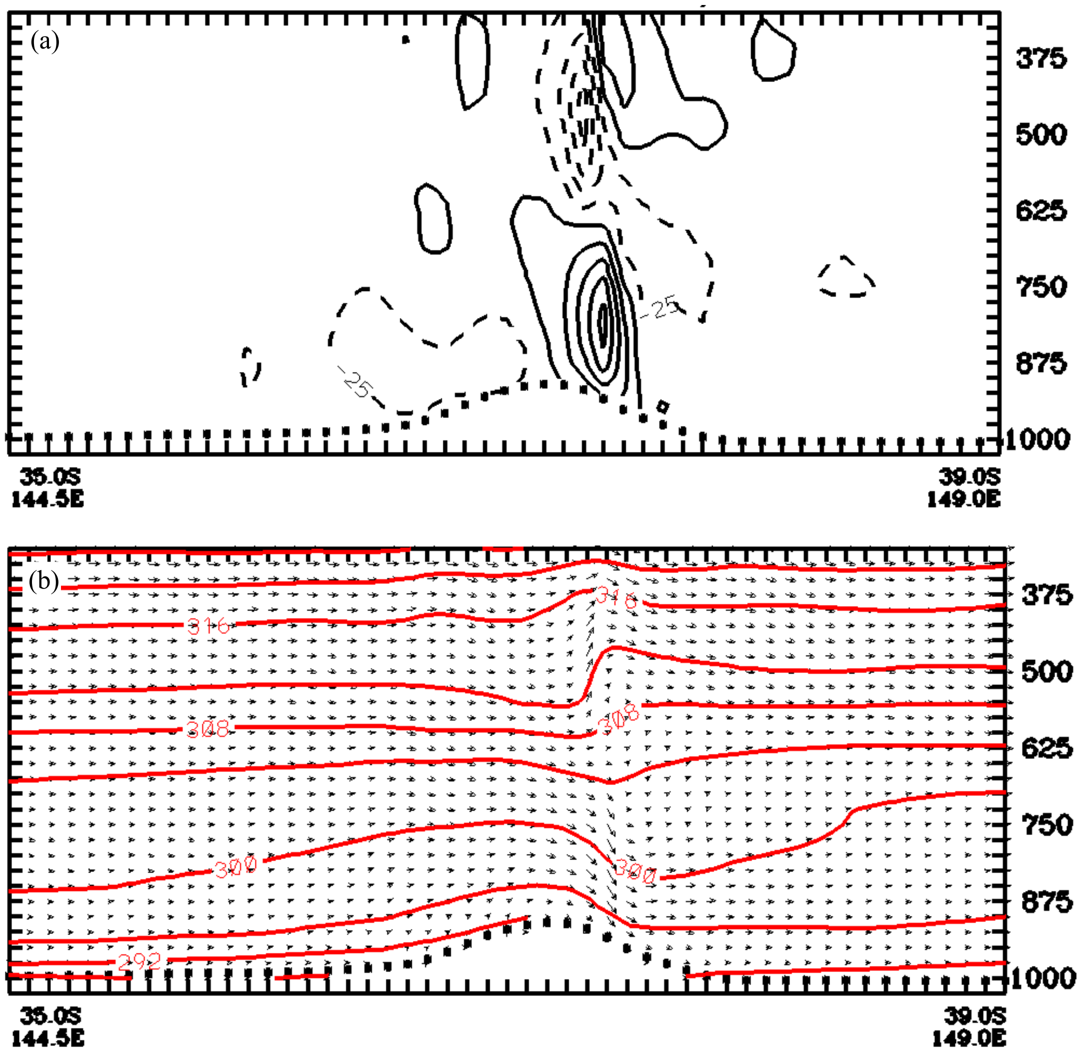

(a)
375
500
625
750
875
1000
-25
-25
35.0S
144.5E
39.0S
149.0E
(b)
316
316
308
308
300
300
292
375
500
625
750
875
1000
35.0S
144.5E
39.0S
149.0E

Figure 15.